INVITED PAPER

Land-Cover Mapping by Markov Modeling of Spatial–Contextual Information in Very-High-Resolution Remote Sensing Images

Markov random fields (MRFs) are a powerful and flexible family of stochastic models for spatial–contextual information in image processing and analysis. In this paper, the use of MRFs for classification of very-high-resolution remote sensing images is reviewed.

By Gabriele Moser, *Member IEEE*, Sebastiano B. Serpico, *Fellow IEEE*, and Jón Atli Benediktsson, *Fellow IEEE*

ABSTRACT | Markov models represent a wide and general family of stochastic models for the temporal and spatial dependence properties associated to 1-D and multidimensional random sequences or random fields. Their applications range over a wide variety of subareas of the information and communication technology (ICT) field, including networking, automation, speech processing, genomic-sequence analysis, or image processing. Focusing on the applicative problem of land-cover mapping from very-high-resolution (VHR) remote sensing images, which is a relevant problem in many applications of environmental monitoring and natural resource exploitation, Markov models convey a great potential, thanks to their capability to effectively describe and incorporate the spatial information associated with image data into an image-classification process. In this framework, the main ideas and previous work about Markov modeling for VHR image classification will be recalled in this paper and processing results obtained through recent methods proposed by the authors will be discussed.

KEYWORDS | Data fusion; land-cover mapping; Markov models; Markov random fields; remote sensing image classification

I. INTRODUCTION

The availability of satellite images, granted by recent and forthcoming missions for Earth observation (EO), currently offers a unique spatially distributed and temporally repetitive capability to observe the Earth's surface at the desired global, regional, or local spatial scale. Spaceborne passive sensors collect multispectral images (i.e., images made of several channels, each represented by a gray-level image and associated to a given wavelength range) with resolutions ranging from a few kilometers to less than one meter [1]. Satellite active microwave imaging systems, based on the synthetic aperture radar (SAR) technology, can acquire images regardless of solar illumination and cloud cover conditions and the latest SAR constellations reach up to metric resolution with revisit times as short as 12 h. In particular, the spatial resolutions of satellite imagery have systematically improved during the past three decades: images with 1–4-m (or finer) resolution

Manuscript received February 6, 2012; revised May 3, 2012; accepted July 13, 2012. Date of publication September 17, 2012; date of current version February 14, 2013. This work was supported by the Italian Space Agency under the "OPERA—Civil protection from floods" project.

G. Moser and **S. B. Serpico** are with the Department of Telecommunications, Electronic, Electrical, and Naval Engineering (DITEN), University of Genoa, Genoa I-16145, Italy (e-mail: sebastiano.serpico@unige.it).

J. A. Benediktsson is with the Faculty of Electrical and Computer Engineering, University of Iceland, Reykjavik 101, Iceland (e-mail: benedikt@hi.is).

Digital Object Identifier: 10.1109/JPROC.2012.2211551

from spaceborne sensors (e.g., IKONOS, QuickBird, WorldView-2, GeoEye-1) have become popular for civil applications in the last ten years. Such very-high-resolution (VHR) images provide plenty of detailed information about the ground on a regular basis for applications such as urban planning, precision farming, or risk mitigation and damage assessment for environmental disasters.

In these applications, the opportunity to map the land cover of the observed area from the available satellite data is especially relevant. Indeed, EO-based generation of land-cover maps is feasible thanks to the use of supervised image-classification techniques that are framed within the pattern recognition discipline [1], [2]. Pattern recognition offers a comprehensive methodological framework to formalize and address the estimation of the land cover of the ground area corresponding to each pixel in an input satellite image, given a predefined and suitably characterized collection of land-cover classes [2], [3]. Specifically, when medium or coarse resolutions (i.e., approximately 30 m or coarser) were considered, a number of noncontextual classification techniques, based on methodological approaches drawn from Bayesian decision theory [2], neural networks [4], fuzzy logic [5], support vector machines (SVMs) and kernel-based learning [6], or multiple-classifier systems [7], have been proposed and experimentally found effective in many applications. Noncontextual classifiers estimate the land cover associated with each pixel *per se*, regardless of the land-cover estimates computed for the other image pixels [1]. Such an approach offers the advantages of conceptual and computational simplicity but neglects the information associated with the usually strong correlation among neighboring pixels in real-world imagery [8]. Indeed, neighboring pixels, provided they are not separated by an edge between two homogeneous image regions, are likely to share the same class label: noncontextual classifiers do not take benefit of this information in the classification process.

When switching to VHR imagery, especially when acquired over urban or built-up areas, ground objects or structures made of different materials can be well appreciated [1], [9], whereas, when imaged at coarser resolution, the spectral responses of ground objects and related materials are averaged together over the larger ground area associated with each pixel. These materials may include concrete, asphalt, metal, plastic, glass, water, grass, wood, bare soil, etc., and be arranged into complex configurations in the image. The appreciable presence of the distinct spectral responses of these materials makes the spatial behaviors of the pixel intensities in VHR imagery much more heterogeneous than at coarser resolution (although VHR multispectral sensors usually acquire a small number, generally 3–4, of spectral channels). Furthermore, a well-defined geometrical structure can often be appreciated in VHR images including certain land covers, such as urban (streets, buildings, etc.) or agricultural areas (cultivated fields). Consequently, VHR images offer better potential for detailed and accurate land-cover classification, but the complex nature of the related satellite observations makes the discrimination of distinct thematic classes a much more challenging task.

Due to these spatial properties of VHR imagery, noncontextual supervised classification techniques, which were consolidated in the analysis of coarser resolution images, are expected to be considerably less effective when applied to VHR data. Contextual classification methods, which explicitly incorporate information on the spatial context of each pixel in the estimation of the related land cover, are needed to cope with the heterogeneity of the spatial field of VHR observations and to correctly capture the related spatial–geometrical information [1], [9], [105].

In this framework, Markov random fields (MRFs) play a primary role [10], [11]. They conceptually generalize the notion of Markov chain, a popular model for 1-D random sequences in many applications (queueing [12] and scheduling systems [13], telecommunications [14], speech and audio processing [15], tracking [16], document recognition [17], etc.), to the 2-D framework of image modeling [18], analysis [11], and compression [19]. MRFs are a general family of probabilistic models for 2-D stochastic processes defined over discrete pixel lattices [11]. They represent flexible and powerful models for the spatial–contextual information associated with images [10], [20], [21] and their use in classification allows taking advantage of the dependence among neighboring pixels to maximize the accuracy in land-cover discrimination.

The theory of MRFs is rooted in the general frameworks of image processing and pattern recognition. However, such models currently play an especially important role in remote sensing. As also mentioned above, the spatial behaviors of remote sensing data can vary widely with the spatial resolution, the season, the illumination level, the typology of observed scene (e.g., urban, agricultural, forested area), etc. On the one hand, spatial models based on prior information on the shapes and geometrical structures of the target classes, which are quite popular in computer vision and industrial vision, are likely too restrictive in remote sensing. On the other hand, MRFs characterize, in a mathematically rigorous way, the relationships between local and global properties of the image statistics on a per-pixel basis [20], [21] and are generally flexible enough to characterize, for classification purposes, the contextual information associated with remote sensing data. They also exhibit a considerable flexibility in incorporating not only spatial context but also multiple information sources [22].

These properties explain their success in many image analysis problems in remote sensing, including classification [23]–[26], segmentation [27]–[29], restoration [30], denoising [31], visualization [32], feature extraction [33], edge detection [34], road extraction [35], subpixel analysis [36], change detection [37]–[40], multitemporal classification [41], data mining [42], microwave imaging [43], SAR interferometry [44], radargrammetry [45], image

fusion [46], decision fusion [47], building detection [48], data assimilation [49], and super-resolution mapping [50], [51]. MRF-based classification has recently gained even greater attention also because computationally efficient approaches (e.g., graph cuts [52], [53]) to the related complex minimization problems were developed and successfully applied.

Advanced MRF-based techniques for land-cover classification from remote sensing data can be very powerful and complex; include sophisticated hierarchical [54], multiresolution [55], [56], or multiscale models [57], [58]; and involve challenging computational problems. However, the current development of this research area also offers effective automatic parameter-optimization algorithms, whose applications make the use of Markovian classifiers feasible also for end users with no deep image processing knowledge. This capability to pair up conceptual complexity and ease of use, together with classification accuracies and execution times well matching the requirements of land-cover mapping applications, suggests a strong scientific maturity of the field of MRF-based classification and, more generally, of the image processing discipline.

In this paper, we focus on the use of MRF models in the framework of land-cover classification from remote sensing images, especially when acquired by VHR sensors. The key ideas about MRFs are recalled and their use to characterize the contextual information associated with a VHR image is discussed. The remarkable capability of MRFs to also incorporate information from further approaches to spatial modeling is investigated. In particular, the opportunity to characterize through MRFs the information associated not only with the correlations among neighboring pixels but also with the presence of edges between distinct land covers, homogeneous image regions (or segments), and textured image areas is discussed. To this end, recent approaches developed by the authors are recalled and applied to selected case studies to experimentally demonstrate and exemplify the potential of Markov models in remote sensing image classification [59]–[61]. Further review papers that discuss the use of MRF models in remote sensing can be found in [21] and [65].

The paper is organized as follows. A general discussion on land-cover mapping from EO images and on the related role of spatial information modeling is reported in Section II. The key ideas about MRFs and examples of MRF-based methodologies for VHR image classification are discussed in Section III. Case studies and experimental examples are presented in Section IV and conclusions are drawn in Section V.

II. LAND-COVER MAPPING FROM REMOTE SENSING: THE ROLE OF SPATIAL INFORMATION

Within a pattern recognition framework, the task of mapping land cover from remote sensing imagery can be formalized as a supervised image-classification problem [1]. Such a problem has been investigated for some decades, involving progressively increasing spatial and spectral resolutions [1]. Thanks to the current advances in this research area, together with the computing capabilities offered by contemporary hardware and software architectures, the application of complex remote sensing image-classification techniques is now feasible not only for laboratory experiments but also when operational, computational, and accuracy requirements are dictated by practical applications.

A probabilistic framework is usually adopted to formulate most classification techniques. The input image and the output classification map are modeled as realizations of 2-D random processes $x(m,n)$ and $y(m,n)$ ($m = 0,1,\ldots,M-1$; $n = 0,1,\ldots,N-1$) defined over the same rectangular $M \times N$ pixel lattice $I = \{(m,n) : m = 0,1,\ldots,M-1; n = 0,1,\ldots,N-1\}$. The process x is typically vector valued and maps each pixel (m,n) to the multidimensional random vector $x(m,n)$ of all related remote sensing observations. The process y is discrete and maps each pixel (m,n) to a class label $y(m,n)$ taking values in a predefined finite set of C land-cover classes [1], [2]. In pattern recognition terminology, the components of $x(m,n)$ are called features, $x(m,n)$ is the feature vector of pixel (m,n), and the multidimensional space whose coordinates are the features is the feature space. For example, the observations of a multispectral sensor in different wavelength ranges are often used as features for classification [1], [3].

A supervised image-classification method aims at computing an estimate $\hat{y}(m,n)$ of the stochastic process $y(m,n)$ such that the probability that $\hat{y}(m,n) \neq y(m,n)$ (probability of error) is minimized. To this end, a subset of pixels, named training pixels, whose true class labels are *a priori* known, is supposed to be available. Indeed, the adjective "supervised" actually indicates the use of such training information, which may practically derive from *in situ* campaigns or be visually identified in the considered image by a photo-interpreter [3]. Training pixels conceptually represent "examples of the classes" and are used to describe prior knowledge on the statistical behaviors of the feature vectors belonging to each class [2], [3]. Indeed, the key scientific challenge, which is intrinsic in a supervised image-classification problem, consists in the need to properly "generalize" from a finite (and often small) set of preclassified training pixels a reliable "model" for the unknown statistical relationship between the feature-vector and the class-label stochastic process.

For a thorough discussion of such generalization concepts we refer to [6]. Here, we focus more closely on the role of spatial information modeling in this classification framework. Noncontextual methods address a classification task by accepting an additional simplifying assumption, i.e., the pairs $(x(m,n), y(m,n))$ of input/output variables associated with distinct pixels are independent of one another. This condition is conceptually analogous to

a whiteness assumption in random-noise modeling and obviously favors analytical tractability and computational simplicity. Nevertheless, it is violated by real images, in which neighboring pixels generally exhibit high correlations [8]. On the contrary, contextual approaches to classification do not state this assumption and consequently need to properly model, in the classification process, the correlations among neighboring pixels or, more generally, the spatial information associated with the image data. This approach is intrinsically more complex than the noncontextual one, but, as discussed in Section I, is often mandatory when a VHR image is to be classified, due to the need to handle both the spatial heterogeneity and the geometrical properties associated with the input data.

From this perspective, three main methodological approaches can be recalled to incorporate spatial information in image analysis, i.e., MRF modeling, texture extraction, and region-based or object-based methods. MRF-based techniques will be more extensively discussed in Section III. Here, we briefly recall the key ideas of the other two approaches.

The concept of texture in image analysis aims at formalizing the intuitive notion of the presence, in a given region of an input image, of a rather repetitive behavior in the spatial distribution of the pixel intensities [8]. Typical examples may be urban or forested areas in high-resolution imagery, in which rather repetitive spatial structures are due to the distributions of buildings and tree canopies, respectively, in the imaged scene. Texture-extraction (or texture-analysis) methods compute a set of transformed features that are related with the spatial relationships among the intensities of neighboring pixels. For classification purposes, these features can be used together with or in place of the original remote sensing observations [1], [8]. Among well-known approaches to texture analysis, we recall Haralick's features, which characterize the joint local statistics of pairs of pixels through the so-called gray level co-occurrence matrix [1], [66], [67]; the semivariogram, which is a spatial second-order statistics of the pixel intensities (see also Section IV-B) [68]; mathematical morphology, which is based on a family of nonlinear operators related with Minkowski's set theory [69]–[73] and allows capturing geometrical and multiscale properties of the image through morphological profiles [71], [72] or morphological attribute filters [73]; continuous-valued Markov models, which provide a parametric characterization of the joint statistics of the pixel intensities [33]; wavelet transforms [74], [75] and Gabor filters [76], which compute a set of features through suitable linear filters aimed at capturing multiscale and directional properties of the image. Several works have demonstrated the contribution of such additional texture features to discriminating differently textured land covers in remote sensing images [67]–[73]. However, most texture-extraction methods involve moving-window procedures, i.e., the texture features of each pixel are computed by processing the image samples included in a square or rectangular window centered on the pixel itself [8]. Consequently, a common drawback is that artifacts and unreliable classification results are often obtained near the spatial edges between distinct land covers.

A further interesting approach is represented by region-based and object-based methods that rely on the combination of classification and segmentation algorithms [77]. A segmentation technique aims at splitting an image into a set of homogeneous regions (or segments), often corresponding to objects or portions of objects [8]. Many approaches have been proposed to address this problem, including region-growing algorithms, which progressively expand a collection of segments starting from a suitable set of seed points [8]; Markovian methods, which formulate segmentation as an unsupervised classification problem addressed through an MRF model [27]–[29]; fuzzy-connectedness techniques, which formalize the uncertainty associated with image data through fuzzy theory [78], [79]; watershed methods, which represent the field of the pixel intensities as a topographic relief and search for the related catchment basins [80], [81]; and hierarchical algorithms, which generate a hierarchy of segmentation results associated with progressively increasing spatial detail [58], [82], [83]. A segmentation map intrinsically offers a characterization of the geometrical structure associated with the image, a property that explains the current relevance of region-based techniques in VHR image analysis. A simple intuitive region-based classifier could just label each segment as a whole rather than separately classifying each pixel. However, more sophisticated methods have been developed by properly combining segmentation, feature extraction, and possibly multiscale analysis [77], [84]. Such approaches optimize the discrimination of classes characterized by strong geometrical information (e.g., agricultural fields, urban areas). Nevertheless, they may be rather inadequate for textured classes with no well-defined geometrical structure (e.g., dense forested areas).

III. MARKOV RANDOM FIELD MODELING FOR VHR IMAGE CLASSIFICATION

A. Markov Random Fields for Image Classification

Let us synthetically denote the coordinate pair (m, n) of a generic pixel by a single subscript i $(i \in I)$, write simply x_i and y_i instead of $x(m, n)$ and $y(m, n)$, respectively, and indicate by $p(\cdot)$ and $P(\cdot)$ probability density functions of continuous random vectors and probability mass functions of discrete random variables and vectors. Let us also collect all the x_i $(i \in I)$ variables, i.e., all the feature vectors in the input image, in a unique random vector X, and all the y_i $(i \in I)$ variables, i.e., the land-cover labels of all pixels in the output land-cover map, in a unique discrete random

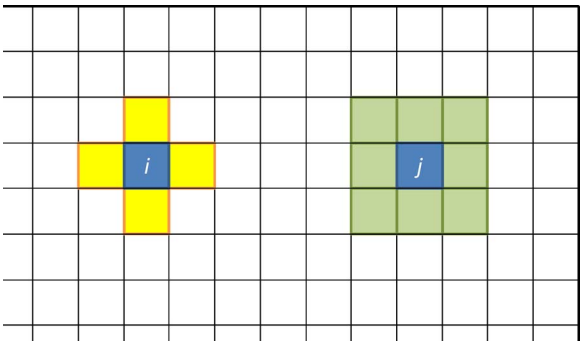

Fig. 1. *Examples of neighborhoods: The black lines denote the pixel lattice, the yellow pixels constitute the first-order neighborhood of the ith pixel, and the green pixels constitute the second-order neighborhood of the jth pixel.*

vector Y. The Bayesian maximum *a posteriori* (MAP) rule recommends searching for the map Y^* that maximizes the posterior probability mass function $P(Y|X)$ [2]. As a well-known result from Bayesian decision theory, this global MAP criterion exhibits important analytical properties, as it minimizes the probability of classification error [2], but its formulation is computationally unfeasible due to the huge number of discrete variables to be jointly optimized (i.e., the MN components of the vector Y).

The MRF approach offers a computationally efficient solution to this difficulty by passing from a global model for the joint posterior distribution of all the class labels, conditioned to all observations, to a local model based on a neighborhood system [10]. We assume that, for each pixel, a well-defined neighborhood is introduced and we write $i \sim j$ to indicate that pixels i and j are neighbors $(i, j \in I)$ [10]. The most typical examples are the first- and second-order neighborhoods that include, for each pixel $i \in I$, the four adjacent and the eight surrounding pixels, respectively (see Fig. 1). The 2-D stochastic process of the class labels is an MRF with respect to this neighborhood system if its probability mass function $P(Y)$ is strictly positive for all label configurations Y and if the following Markovianity condition holds for all pixels $i \in I$ [20]:

$$P(y_i|y_j, j \neq i) = P(y_i|y_j, j \sim i). \tag{1}$$

This means that the probability distribution of the class label of each pixel i, conditioned to the labels of all other image pixels, can be restricted to the distribution of the label of i, conditioned only to the labels of its neighboring pixels [10]. The strict positivity of $P(Y)$ is essentially a technical assumption, required to ensure analytical tractability. As mentioned in Section I, the Markovianity property extends to the 2-D pixel lattice I the usual definition of Markov chain for 1-D sequences [18]. A thorough analytical discussion of this property and of its relationship with similar properties for (1-D and 2-D) Markov processes can be found in [11].

The MRF hypothesis has a crucial impact on the problem of land-cover mapping. Indeed, thanks to the so-called Hammersley–Clifford theorem [20], [21], it is possible to prove that, under mild assumptions, if Y is an MRF, then the global posterior probability can be written as the following Gibbs distribution:

$$P(Y|X) = \frac{e^{-U(Y|X)}}{Z(X)} \tag{2}$$

where the function $U(Y|X)$, called energy function, is defined locally, according to the neighborhood system, and $Z(X)$, usually named partition function, is a normalization factor [10], [20]. Here, the word "energy" is used by formal analogy with certain probabilistic models employed in statistical mechanics and thermodynamics [85].

Therefore, the maximization of the global posterior probability mass function $P(Y|X)$ is equivalent to the minimization of the energy function $U(Y|X)$. Thanks to the local, neighborhood-based definition of the energy, this minimization problem is computationally tractable [10], [21], a remarkable result that offers a feasible solution to the otherwise intractable problem of global MAP image classification and explains the widespread success of MRF-based approaches in remote sensing.

A basic example of an MRF energy, which has been widely used for medium-resolution remote sensing image classification, is the following function [10], [22], [25]:

$$U(Y|X) = -\sum_{i \in I} \ln p(x_i|y_i) + \beta \sum_{i \sim j} \left[1 - \delta(y_i, y_j)\right] \tag{3}$$

where $\delta(\cdot)$ is the Kronecker function (i.e., $\delta(a, b) = 1$ for $a = b$ and $\delta(a, b) = 0$ otherwise) and β is a positive parameter. In (3), we implicitly assume that the features are continuous random variables. The energy function in (3) is expressed as a linear combination of two contributions. The first contribution is related to pixelwise information and is formulated in terms of the probability density function of the feature vectors conditioned to the related class labels. This probability density can be estimated class by class, based on the available training pixels (a discussion of the main parametric and nonparametric approaches to this estimation problem can be found in [2]). The minimization of only this first energy contribution by itself would be equivalent to a noncontextual Bayesian classification of the image [2]. Compared to this scenario, the inclusion of the second term allows the spatial context of each pixel, expressed in terms of its neighborhood, to be taken into account in the classification. When minimizing $U(Y|X)$

with respect to Y, this second term (often known as Potts model or multilevel logistic model [10]) penalizes spatial transitions among neighboring pixels with different class labels, thus favoring, in the output classification map, the generation of connected regions associated with the same land-cover class. This behavior is consistent with the usually high correlation between the class labels of neighboring pixels and favors a high accuracy in discriminating spatially homogeneous land covers. The parameter β tunes the reciprocal weight between the pixelwise and contextual terms.

More sophisticated models can be devised to incorporate, into the classification process, not only information about the homogeneity of connected regions belonging to the same land cover but also information associated to spatial edges, geometrical structures, anisotropic spatial behaviors, multiscale processing, etc. [10]. Examples of such approaches will be discussed in the Sections III-B and III-C. Here, we only point out that there is a large freedom in the choice of an energy function that fits the requirements of the considered classification problem and the characteristics of the target land-cover classes. This scenario makes the family of MRF models very flexible and allows for their practical use in diverse applications involving land-cover mapping from EO data.

This flexibility is confirmed by the fact that the MRF approach can be further extended to integrate not only pixelwise and neighborhood information but also multiple input information sources [22]. Similarly to (3), in which the energy function is a weighted sum of two contributions associated to pixelwise statistics and spatial context, the Markovian approach can benefit from multiple information sources through the definition of the energy function as a linear combination of several contributions,[1] each related to one information source [22]. The minimization of the resulting energy intrinsically fuses the information conveyed by the input sources in the classification process. Such a Markovian approach to multisource fusion, which also bears similarities to opinion-pool consensus approaches to decision fusion [86], has been successfully applied in a number of remote sensing applications, involving multisensor [87], multitemporal [41], multiresolution [55], and multichannel imagery [37], and further confirms the power of this family of stochastic image models.

As mentioned above, the use of an MRF makes the problem of global MAP classification tractable. Currently, this statement is especially interesting, thanks to a number of computational developments that have received a strong attention in the last decade. Indeed, two classical iterative approaches to MRF energy minimization are: simulated annealing (SA), a well-known stochastic method that may converge, under suitable assumptions, to the global energy minimum and usually involves long computation times [20], [88]; and iterated conditional mode (ICM), a deterministic method that usually exhibits short execution times, but converges only to a local energy minimum and may be sensitive to initialization [22], [89]. A number of alternate approaches have been proposed (see [10] for a thorough review), also pursuing the opportunity to exploit parallel processing [54]. Recently, a strong focus has been given to graph-cut methods that formulate the energy-minimization problem as a maximum-flow problem over a suitable graph [52]. Graph cuts usually exhibit acceptable computation times and are proven to converge to a global energy minimum in the case of binary classification (i.e., $C = 2$) [52] and to a "strong" local minimum (i.e., a local minimum endowed with good optimality properties) when more than two classes are involved [53]. The availability of such computationally efficient tools, together with the aforementioned flexibility of the family of MRF models and with the recent developments in hardware and software, currently make the Markovian approach a scientifically mature and powerful strategy for land-cover mapping from remotely sensed imagery.

B. Modeling Edges and Multiple Spectral Responses in a Markovian Classifier

As mentioned in Section III-A, basic MRFs such as the Potts model were found satisfactory in the case of medium and coarse resolution input images, but may be insufficient for VHR imagery. The main reasons are that: 1) at moderate or coarse resolution, land covers generally look quite homogeneous, whereas each land-cover class in a VHR image is actually a collection of subclasses related to the spectral responses of different materials (see Section I); 2) the spatial smoothing favored by Potts-like MRFs may penalize the classification accuracy around the edges between different land-cover classes or near small-scale details. Both issues are especially important, for example, for images acquired over urban areas.

More advanced MRF models are needed to correctly characterize the information associated with class edges and with the presence of the spectral responses of multiple materials in VHR imagery. To further point out the potential of MRF modeling also in this challenging setting, we recall a recently proposed approach that explicitly addresses both issues 1) and 2) [60]. The key idea of the method is to introduce an MRF model that combines information about land-cover classes (characterized by training data), about material subclasses, identified by a noncontextual clustering algorithm, and about edges. A noncontextual clustering method aims at partitioning the set of the feature vectors associated with the image pixels into several subsets, which are called clusters and represent "natural groups" of samples in the feature space [1]. The ground materials that can be appreciated in the input VHR image are expected to be well discriminated through their spectral responses. Hence, noncontextual clustering is applied in the feature space by implicitly assuming that

each resulting cluster may be associated with the spectral response of a given material. Many noncontextual clustering methods have been proposed, ranging from basic procedures, such as k-means [1], to much more sophisticated statistical [2], fuzzy [5], or neurofuzzy methods [4].

A well-known approach to the modeling of edges in MRFs is represented by line processes [10], [20], [22]. A line process is an additional discrete-valued (usually binary) random field, coupled with the random field of the class labels and possibly defined over a suitable dual lattice. The line-process field basically denotes the presence and locations of edges and can be used to prevent spatial transitions between different class labels across an edge to be erroneously penalized by MRF-based processing [10]. This favors at the same time spatial regularization inside connected image areas and correct preservation of the boundaries between distinct land covers. An alternate approach to favor edge preservation would be to use adaptive MRF models, in which the spatial energy contribution is tuned according to the local image statistics and the likelihood that an edge is present. For instance, adaptive neighborhood systems could be used to match the shape of the neighborhood of each pixel with possible linear or geometrical structures [29], [31], [90], or the weight parameter of the contextual energy term [e.g., β in (3)] could be tuned on the basis of the local image statistics [82], [91].

As a simple formalization of the "edge-preserving" Markovian classifier in [60], which is based on the line-process approach, we associate, with each pixel $i \in I$, a binary edge label w_i, such that $w_i = 1$ if an edge passes through the pixel and $w_i = 0$ otherwise, and a cluster label z_i that indicates to which cluster the pixel belongs in the noncontextual clustering result. According to the Markovian approach to data fusion, an energy function can be defined as a linear combination of distinct contributions to integrate the relationships between land-cover classes, their spectral subclasses, and edges in the classification process, i.e.,

$$U(Y,Z,W|X) = -\sum_{i\in I} \ln p(x_i|z_i) + \beta \sum_{i\sim j} \left[1-\delta(y_i,y_j)\right] \times \delta(w_i,w_j) + \gamma \sum_{i\in I} E(w_i|w_j, j\sim i) \quad (4)$$

where β and γ are positive weight parameters.

Similar to (3), the first energy contribution is associated with pixelwise information, formalized in terms of the conditional statistics of the feature vectors. However, unlike (3), the statistics conditioned to clusters and not to land-cover classes are used here to take into account the presence of the spectral responses of multiple materials per each class. Analogously to the MRF model in (3), the probability density function of the feature vector conditioned to each cluster can be estimated by applying a parametric or nonparametric method to the pixels that belong to the cluster. Because each cluster is assumed to be associated with the spectral response of a ground material, a parametric monomodal model may often fit well the statistics of the feature vectors in the cluster. The second energy term is associated with spatial–contextual information and aims at penalizing, in the minimum-energy decision rule, each spatial transition inside the neighborhood between different class labels, provided no edge is located between them. This choice aims at encouraging spatial continuity of the areas assigned to the same thematic class without oversmoothing the related borders. On the contrary, no penalty is desired for a pair of different neighboring class labels, when they are separated by an edge. The third term is aimed at penalizing undesired edge configurations, in order to favor edge continuity, prevent isolated edge pixels, and ensure rotational invariance of the edge energy contribution. For each pixel $i \in I$, it is expressed in terms of the function $E(\cdot)$, which depends on the related edge label w_i and on the edge labels of the neighboring pixels. A lookup table can be used to define the value of $E(\cdot)$ associated with each edge-label configuration in the neighborhood. For instance, when a second-order neighborhood is used (see Fig. 1), a simple choice (adopted in [60]) could be as follows: 1) when $w_i = 1$, the desired neighborhood configurations are those in Fig. 2(a) and are assigned zero value of the function $E(\cdot)$, whereas all other configurations are given a predefined large value to penalize them; and 2) when $w_i = 0$, zero value is assigned to $E(\cdot)$ for the desired neighborhood configurations in Fig. 2(b), a small penalty is associated with the configurations in Fig. 2(c) (each possibly corresponding to the end point of an edge), and a large penalty is associated with all other configurations.

Concerning the minimization of the energy in (4), we only recall that, since the clusters are aimed at modeling multiple spectral responses within each land cover, suitable constraints involving the Y and Z variables have to be incorporated in the minimization process to correctly capture the relationship among the land-cover classes and their spectral subclasses. The main idea is that, to minimize the function $U(\cdot)$ in (4), for each value of the class label y_i, the minimization is restricted only to the values of the cluster label z_i that are compatible with y_i ($i \in I$) [60], [92]. Further details on the definition of the function $E(\cdot)$ and on energy minimization can be found in [60].

C. Integrating Segment, Multiscale, and Texture Information in a Markovian Classifier

As discussed in Section II, region-based and texture-based methods represent further important tools for land-cover mapping from EO (especially VHR) images and usually well discriminate classes that exhibit a well-defined geometrical structure and a textured spatial behavior, respectively. From this perspective, these approaches to the modeling of spatial information may be complementary to

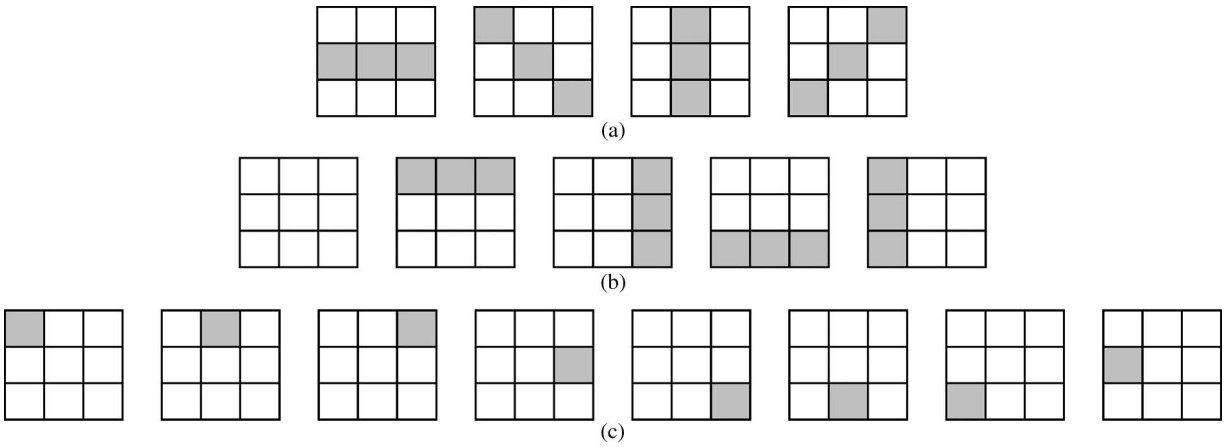

Fig. 2. ***Relevant edge-label configurations in the second-order neighborhood of a generic pixel for the edge-preserving MRF model in (4): The central pixel of the 3 × 3 window is the generic considered pixel; "gray" and "white" denote edge*** $(w_i = 1)$ ***and nonedge*** $(w_i = 0)$ ***pixels, respectively.***

each other and to MRFs, such as the Potts model, that favor the generation of homogeneous areas assigned to the same class.

In particular, multiscale region-based methods represent especially appealing tools. The key concept of these methods is to generate, from the input EO image, a collection of segmentation results corresponding to different spatial observation scales. In a VHR image, it is expected that the main regions and structures in the scene will be identified at coarse scales, whereas smaller structures, objects, and parts of objects will be apparent at fine scales. Multiscale methods aim at taking benefit of this complementary information to capture the spatial–geometrical structure of the scene, a strategy that bears analogies with computer vision approaches used, for instance, in robotics or video surveillance.

To exemplify the flexibility of MRFs as spatial modeling tools, we recall here two recently proposed techniques that aim at integrating the Markovian, region-based, and texture-based approaches to image classification in a unique multiscale methodology [59], [61]. Focusing first on the combination of the MRF- and region-based strategies, the key idea is to extract multiscale information by a segmentation technique and to use the data fusion capabilities of MRFs to incorporate this information in the classification process [59]. Given the VHR image to be classified, a multiscale segmentation method is applied to generate a collection of K segmentation maps, including both coarse-scale maps, highlighting the main regions in the image, and fine-scale maps, detecting smaller regions and structures. Each segmentation map is thought of as a distinct information source, thus formalizing the classification task as a data fusion problem addressed by MRFs [59]. In accordance with the Markovian approach to data fusion, the energy function is expressed as a linear combination of energy contributions, each related to the information conveyed either by the spatial neighborhood of each pixel (through the Potts model) or by each segmentation map, i.e.,

$$U(Y|S) = -\sum_{i\in I}\sum_{k=1}^{K} \alpha_k \ln P(s_{ik}|y_i) + \beta \sum_{i\sim j} \left[1 - \delta(y_i, y_j)\right] \tag{5}$$

where s_{ik} is a discrete variable ("segment label") denoting to which segment the ith pixel belongs in the kth segmentation map ($i \in I$; $k = 1, 2, \ldots, K$); S is a discrete random vector collecting all such segment-label variables; and α_k and β are positive parameters. The choice to formulate the energy contribution related to the kth segmentation map in terms of the pixelwise probability mass function $P(s_{ik}|y_i)$ of the related segment labels, conditioned to the class label [see (5)], is inspired by the similar definition of the classical pixelwise energy term $[-\ln p(x_i|y_i)]$ [see (2)] associated with the probability density function of a feature vector, conditioned to the class label. This choice is equivalent to considering the segment labels as features, each characterizing one of the information sources fused by the MRF, and allows the statistical relationships between land-cover classes and segmentation maps at different scales to be incorporated in the data fusion process. Details on the estimation, from training pixels, of the class-conditional probability mass functions of the segment labels in (5) can be found in [59].

However, if highly textured land covers are present within the classes to discriminate, the described approach might be inappropriate and the integration of texture features may become necessary. To this end, a basic strategy could be to apply an arbitrary texture extraction method, to

stack the resulting features together with the satellite observations, and to apply the described multiscale MRF/region-based approach to the resulting stacked feature vector [1]. However, this procedure would likely be affected by the edge artifacts introduced by the moving-window procedures involved in the texture-extraction stage. To prevent this behavior, more sophisticated combinations of texture extraction, segmentation, and MRF modeling can be devised. In particular, we mention the recently proposed technique in [61] that incorporates texture analysis in the aforementioned region-based multiscale algorithm and adaptively tunes the shape of the moving window according to the edges between the classes, to prevent mixing statistical populations related to distinct land covers in the computation of texture features. The method is iterative and alternates until convergence of two processing steps: 1) the texture features are extracted adaptively to the class edges in the current classification map; and 2) the map itself is updated by applying the described region-based Markovian classifier to both the spectral channels and the current texture features. Details on this technique jointly based on MRF, region, and adaptive texture features can be found in [61].

D. Parameter Optimization for Markovian Classifiers

MRF models for image classification often present internal parameters. Examples are the parameters α_k ($k = 1, 2, \ldots, K$), β, and γ in (3)–(5) that weight the single contributions to the energy function, and additional parameters may also be involved inside each contribution. Since the values of all such parameters generally affect the output classification map, estimation techniques to optimally tune them have to be applied prior to or together with energy minimization. On the one hand, this parameter-estimation problem is a challenging one, mostly because well-known Bayesian maximum-likelihood (ML) estimation algorithms [2] are computationally expensive, if not intractable, for most MRF models [93], due to the difficulty in computing the partition function involved in the Gibbs distribution (2). ML estimation of MRF parameters has been essentially restricted to specific categories of MRFs, such as continuous Gaussian [94] or generalized Gaussian [95] fields, for which the ML rule turns out to be analytically feasible.

On the other hand, estimating the parameters of MRF models is also an operationally important problem, because the availability of effective and automatic parameter-optimization tools is a necessary condition for Markovian classifiers to be conveniently applied by nonexpert users. Also from this perspective, the current availability of a number of approaches to address this problem further confirms the maturity of the field of Markovian image analysis and its usefulness for practical land-cover mapping applications.

Reviews of parameter estimation for MRF-based segmentation and classification can be found in [10], [23], [65], and [93]. Here, we just briefly recall that several approaches have been proposed in the context of MRF models for segmentation [96]–[98] or clustering [93]. Monte Carlo simulations have been used to approximate the partition function in the application of the ML approach [96], albeit often with considerable computational burden. Stochastic gradient methods have been proposed to apply the ML criterion by integrating a stochastic sampling step into a gradient ascent procedure [93]. Approximate pseudolikelihood functionals [10], [89], [97] are quite popular because they are numerically feasible and not computationally demanding [37], [38], [55]. However, the resulting estimates are generally not true ML estimates and may often underestimate the spatial interactions unless interpixel correlations are weak enough [93]. The minimum mean square error (MSE) criterion has been used in [99] to formulate the problem of parameter setting as the solution of a suitable system of linear equations.

Comparatively fewer techniques have been specifically introduced for the case of MRF-based supervised image classification. For instance, a genetic algorithm was combined in [100] with simulated annealing to estimate the parameters of an MRF model for multisource classification. The specific problem of estimating the weight parameters in a linear combination of energy terms (such as the aforementioned α_k, β, and γ) was addressed in [41] and [101] by heuristic algorithms and in [23] by a technique based on the Ho–Kashyap numerical procedure. The key idea of this last method (which will be used to optimize the parameters in the experimental examples discussed in Section IV) is to exploit the linear relationship between the energy function and the aforementioned weight parameters to formulate a condition of correct classification of the training pixels as an overdetermined system of linear equations. Then, the numerical solution of this system is addressed through the Ho–Kashyap procedure that is based on an iterative formulation of the MSE criterion [23].

IV. EXPERIMENTAL EXAMPLES

Two relevant case studies are presented. The first one is associated with an IKONOS image acquired over Itaipu, at the border between Brazil and Paraguay. Three channels corresponding to green, red, and near-infrared radiation were available, the spatial resolution was 4 m, and the imaged scene was approximately 8×6 km^2 wide [1999×1501 pixels; see Fig. 3(a)]. A preliminary visual analysis of the image by a photointerpreter remarked that seven main classes were present in the scene, i.e., "urban land," "herbaceous rangeland," "shrub and brush rangeland," "forest land," "barren land," "built-up land," and "water."

The imaged scene represents a challenging classification problem, involving spatially homogeneous classes (e.g., "water") as well as classes with an apparent geometrical structure (e.g., "urban land," "built-up land"), and textured land covers (e.g., the vegetated classes). The

Fig. 3. ***Images used for experiments: RGB false-color compositions of the three multispectral channels of both (a) the IKONOS image (1999 × 1501 pixels) acquired over Itaipu (Brazil/Paraguay border) and of (b) the 330 × 200-pixel subset; (c) RGB true-color composition of three (out of four) channels of the IKONOS image acquired over Alessandria (Italy, 750 × 750 pixels).***

spatial heterogeneity of the urban land cover and the presence of several subclasses can be visually well appreciated in the satellite image [see Fig. 3(a)]. To better focus on the behaviors of the described Markovian approaches to classification, we first considered a smaller subset of the image and then we extended the analysis to the whole image area. The subset [330 × 200 pixels, i.e., around 1.3 × 0.8 km^2; see Fig. 3(b)] was approximately centered on the urban area in the top left part of the image and included all the classes but "built-up land" and "water."

The second case study is associated with an IKONOS image acquired around Alessandria (Italy). The spatial resolution was again 4 m, four channels corresponding to blue, green, red, and near-infrared radiation were available, and the imaged scene was 3 × 3 km^2 wide [750 × 750 pixels; see Fig. 3(c)]. Seven main classes can be visually noted, i.e., "urban and built-up land," "forest land," "water," "wet soil," "bare soil," and two agricultural covers. Also in this case, mapping land cover from this image is a complex problem due to the joint presence of classes

with both a rather well-defined geometrical structure and a textured behavior (e.g., the urban area and the agricultural fields).

In both case studies, all the available spectral channels were used as features for classification and training pixels were collected by photointerpretation.

A. Itaipu Case Study: Image Subset

As a benchmark analysis, we show in Fig. 4(c) the result of the application of a classical noncontextual Bayesian classifier to the "Itaipu" image subset. This classifier was based on a multivariate Gaussian model for the pixelwise statistics of the feature vector and will be referred to as the Gaussian Bayesian classifier in the following. The parameters of the multivariate Gaussian distribution associated with each class were estimated through the corresponding training pixels [2]. We recall that the multivariate Gaussian is a usually accepted model for the class-conditional statistics of the pixel intensities in remote sensing images acquired by passive multispectral sensors [1]. In order to quantitatively evaluate the performance of each classification result, test pixels were collected, again by photointerpretation [see Fig. 4(b)]. Similar to training data, the class labels of the test pixels are *a priori* known but, unlike training pixels, test pixels are not involved in the optimization of the classifier. Instead, they are used to compute numerical accuracy parameters on each considered classification result.

The accuracies obtained by the noncontextual Gaussian Bayesian classifier on this test set (i.e., the percentages of the test pixels of each class that were correctly classified) were rather high for all the considered classes. The overall accuracy (i.e., the percentage of correctly classified test pixels, regardless of their class membership) and the

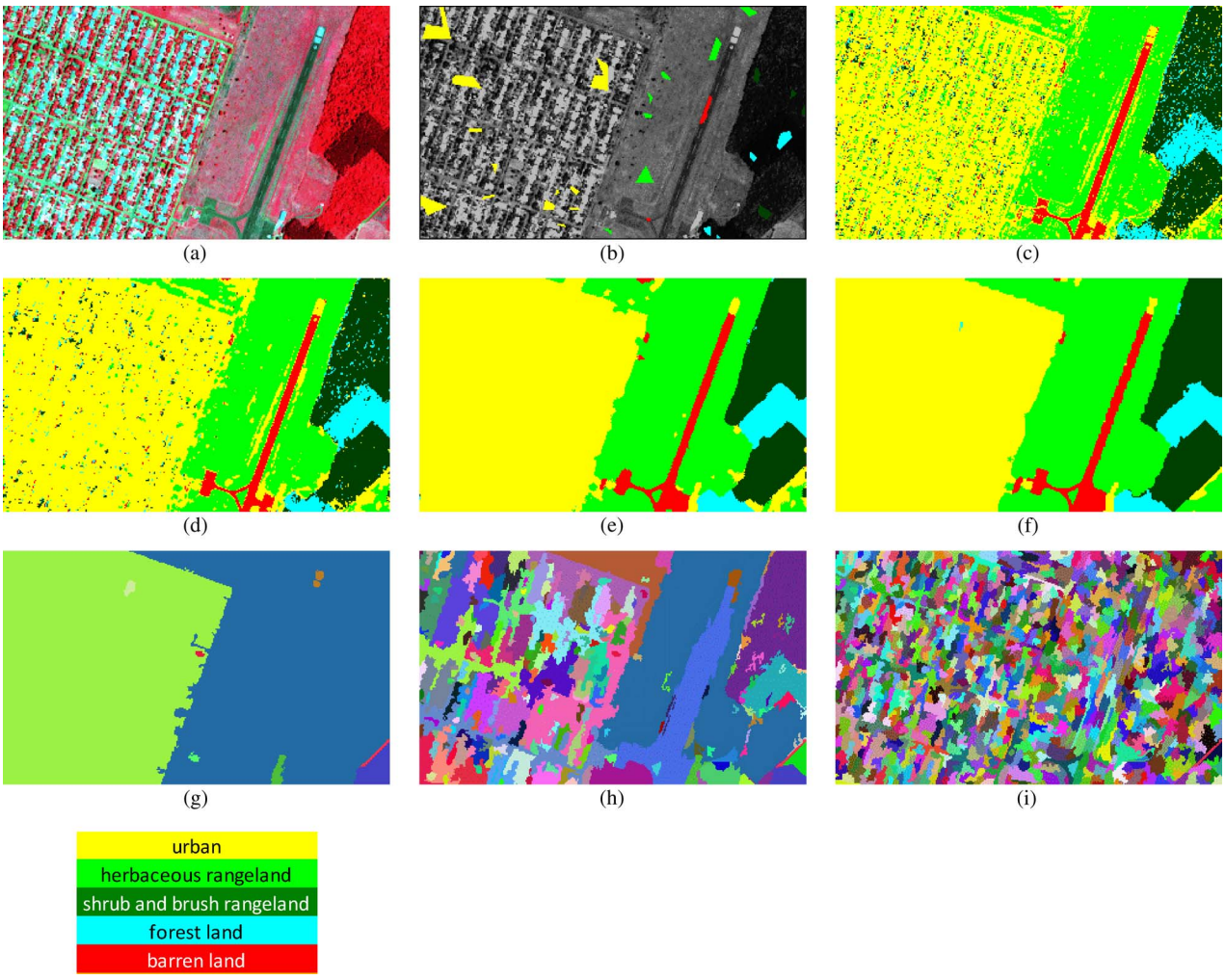

Fig. 4. *"Itaipu" image subset: (a) RGB false-color composition; (b) test map; (c) classification maps obtained by a noncontextual Gaussian Bayesian classifier and (d) by Markovian classifiers based on the Potts model, (e) on the edge-preserving model in (4) and (f) on the multiscale region-based model in (5); (g)–(i) three segmentation maps, corresponding to different scales. Different colors in the segmentation maps in (g)–(i) denote different segments.*

Table 1 "Itaipu" Image Subset: Classification Accuracies (on the Test Set) of the Noncontextual Gaussian Bayesian Classifier and of Markovian Classifiers Based on the Potts Model, on the Edge-Preserving Model in (4) and on the Multiscale Region-Based Model in (5), Respectively

Land cover class	Non-contextual Gaussian Bayesian classifier	MRF-based classifier with Potts model	MRF-based edge-preserving classifier	MRF- and region-based multiscale classifier
urban land	83.5%	94.5%	99.8%	99.8%
shrub and brush rangeland	88.8%	95.6%	100%	100%
herbaceous rangeland	96.9%	99.2%	100%	99.7%
forest land	93.7%	98.9%	100%	100%
barren land	98.9%	100%	100%	100%
overall accuracy	88.3%	96.2%	99.9%	99.9%
average accuracy	92.4%	97.6%	100%	99.9%

average accuracy (i.e., the arithmetic mean of the classification accuracies on the single classes) were approximately 88% and 92%, acceptable values in several applications (see Table 1). However, a visual analysis of the classification map in Fig. 4(c) points out a very noisy spatial behavior, especially over the urban area included in the imaged scene. This result well exemplifies the limited effectiveness of noncontextual classification techniques, when applied to VHR data, and especially the strong impact, on the classification results, of the spatial heterogeneity of the land covers when observed at these resolutions. This is also consistent with the fact that the lowest classification accuracy (around 83%) is obtained for the "urban" class (see Table 1).

In order to illustrate the results that can be obtained with MRF-based classifiers of different complexities, we applied to the considered image subset: 1) the classical Markovian classifier based on the Potts model [see (3)]; 2) the edge-preserving Markovian cluster-based classifier [see (4)]; and 3) the multiscale Markovian region-based classifier [see (5)]. In the case of 1), similar to the noncontextual Gaussian Bayesian classifier, the pixelwise statistics of the feature vector, conditioned to each class, were modeled by a multivariate Gaussian distribution.

With regard to the edge-preserving approach in 2), the hierarchical noncontextual clustering method in [102] was used to identify the subclasses associated with the spectral responses of the ground materials. Inspired by statistical thermodynamics, this clustering method models the collection of feature vectors associated with the image pixels as a thermodynamic system and searches for the clustering solution that minimizes the corresponding free energy [102]. Similar to the previous classifier, also the statistics of the feature vectors conditioned to each cluster [see (4)] were modeled as a multivariate Gaussian distribution [60]. The parameters of this distribution (i.e., the mean vector and the covariance matrix) were estimated as a sample mean and a sample covariance matrix on the pixels that belonged to the cluster [2]. An initial edge map was generated by the Canny edge detector, a well-known technique based on the analysis of the local maxima of the gradient of the input image [8]. Further details on the initialization of the edge-preserving Markovian classifier, on the setting of the parameters of the Canny edge detector, on the application of the clustering method in [102], and on the definition of the relationship between the land-cover class labels and the cluster labels associated with different materials can be found in [9] and [60].

For the multiscale region-based approach in 3), the graph-based region-growing segmentation method in [103] was used and a collection of segmentation maps corresponding to different scales was generated by varying a scale parameter in a predefined range. For instance, three of such maps, ranging from very coarse [Fig. 4(g)] to fine scale [Fig. 4(i)], are shown in Fig. 4. It is worth noting how the urban area was essentially detected as one large region in the segmentation result at coarse scale [Fig. 4(g)] and progressively partitioned into smaller segments, mostly corresponding to objects (e.g., streets, buildings, yards, etc.) or parts of objects, at finer scales [Fig. 4(h) and (i)].

For all the three Markovian methods, in order to minimize the energy functions, the ICM algorithm was chosen as an often acceptable tradeoff between classification accuracy and computational burden. Further details on the initialization of ICM can be found in [59] and [60]. The weight parameters α_k $(k = 1, 2, \ldots, K)$, β, and γ in the linear combinations of energy contributions [see (3)–(5)] were optimized by the method in [23] that formalizes the setting of weight parameters for MRF models as the solution of an overconditioned system of linear inequalities, addressed by the Ho–Kashyap numerical procedure [2]. It is worth noting that, thanks to the application of this method, all considered MRF-based classification procedures are automatic and do not require a user or an operator to perform any manual parameter tuning.

Incorporating spatial–contextual information through the Potts model allowed a nearly 8% increase in the overall accuracy to be obtained, as compared with the result of the noncontextual Gaussian Bayesian classifier (see Table 1). However, the corresponding classification map [see Fig. 4(d)], albeit visually improved as compared with the noncontextual result in Fig. 4(c), still looks quite noisy and affected by the spatial heterogeneity of the input data. In particular, the urban area is not detected as a whole but several isolated subareas are erroneously classified as belonging to either one of the vegetated classes or to "barren

land." On the one hand, these results confirm the advantage of incorporating spatial information in EO image classification, as compared to the use of noncontextual classifiers, and remark the effectiveness of the MRF approach in addressing this spatial modeling task. On the other hand, they also highlight that a basic MRF, such as the Potts model, is insufficient in the challenging setting of land-cover mapping from VHR satellite data.

The application of the edge-preserving MRF-based method defined by the energy function in (4) yielded the classification map in Fig. 4(e), in which the image regions associated with distinct land-cover classes were very effectively discriminated. In particular, the urban area was correctly detected as a whole, even though it is spatially and spectrally very heterogeneous, and the edges among different classes were well identified with no appreciable oversmoothing artifact. This suggests the effectiveness of the discussed Markovian approach in modeling not only the spatial context associated with pixel neighborhoods but also edge information through line processes, land-cover classes defined by the user application, and spectral subclasses associated with the distribution of ground materials in the scene. These results also further confirm the relevance of line processes for edge modeling in MRF-based image processing.

The test-set accuracies obtained by this method were very high, i.e., 99.8% for "urban land" and 100% for the other classes. However, it is worth noting that residual classification errors are still present in the classification map, mostly near the borders between distinct classes. Actually, no test pixels were available in such border areas. This choice is a common practice in remote sensing and is motivated by the need to prevent the inclusion of mixed pixels (i.e., pixels corresponding to ground areas that include multiple land covers) in ground-truth data. This spatial distribution of test pixels explains the very high accuracy values, which were computed on the test set but are clearly optimistic estimates as compared to the accuracy over the whole image area.

Almost identical numerical accuracies were obtained by the multiscale region-based Markovian method based on the energy function in (5) (see Table 1). Nonetheless, a visual comparison of the classification maps generated by this method [see Fig. 4(f)] and by the edge-preserving cluster-based approach [see Fig. 4(e)] points out nonnegligible differences especially near the borders between distinct classes. Such differences did not affect the test-set accuracies because of the aforementioned localization of the test pixels inside homogeneous areas. In any case, a further improvement can be visually noted in the result of the region-based Markovian classifier, as compared with the edge-preserving technique. Both classifiers proved robust against the heterogeneous spatial behavior of the VHR observations, but the Markovian region-based one more accurately identified the borders between the land-cover classes and especially those around the urban area. This is explained by the use of multiscale information, which allows both large- and fine-scale structures to be properly taken into account in the classification process.

More generally, these results further confirm the flexibility of MRF models as contextual classification tools and their adequacy for VHR image analysis. Within this family of stochastic models, the choice of an appropriate MRF formulation and the definition of the related energy function allow spatial information associated with regions, edges, multiple information sources, and multiple scales to be effectively fused for classification purposes.

B. Itaipu Case Study: Whole Image Area

Focusing now on the classification of the whole image area, the application of the region-based multiscale method allowed the classification map in Fig. 5(b) to be obtained. The comments reported in Section IV-A on the accurate detection of the spatial borders between the classes and on the identification of the urban area as a whole hold in this case as well. However, a limitation of this approach is also pointed out by the map in Fig. 5(b). As discussed in Section II, region-based contextual classification techniques are expected to correctly capture the possible spatial–geometrical information associated with certain land-cover classes, but may be inadequate in the application to strongly textured classes with no well-defined geometrical structure. This intrinsic drawback did not critically affect the results obtained on the image subset but is apparent in the map generated from the whole image, in which erroneously labeled areas, especially related to strongly textured classes, such as "herbaceous rangeland" or to "forest land," can be visually noted [see, for instance, the circled area in Fig. 5(b)].

For such classes, a contextual approach that incorporates not only segment but also texture information is desirable. For the sake of comparison, Fig. 5(c) shows the classification map obtained by extracting a set of texture features, by stacking them together with the three satellite spectral channels, and by applying a noncontextual classifier to the resulting compound feature space. In particular, the multivariate semivariogram approach to texture analysis was used. It is based on the computation of a local second-order statistics that can be analytically related to the autocorrelation function of the 2-D stochastic process modeling the input image [68]. The semivariogram has become quite a popular approach for texture extraction from remote sensing images, thanks to its accurate results in several applications and to its limited requirements in terms of parameter tuning [68]. Here, as a noncontextual classifier, we could not use again the aforementioned Gaussian Bayesian method because the Gaussian assumption does not hold for the distributions of texture features. An SVM was used, which relies on the theories of generalization and of kernel-based learning and which is a well-known and widespread technique in the application to remote sensing images [6]. Details on the use of both

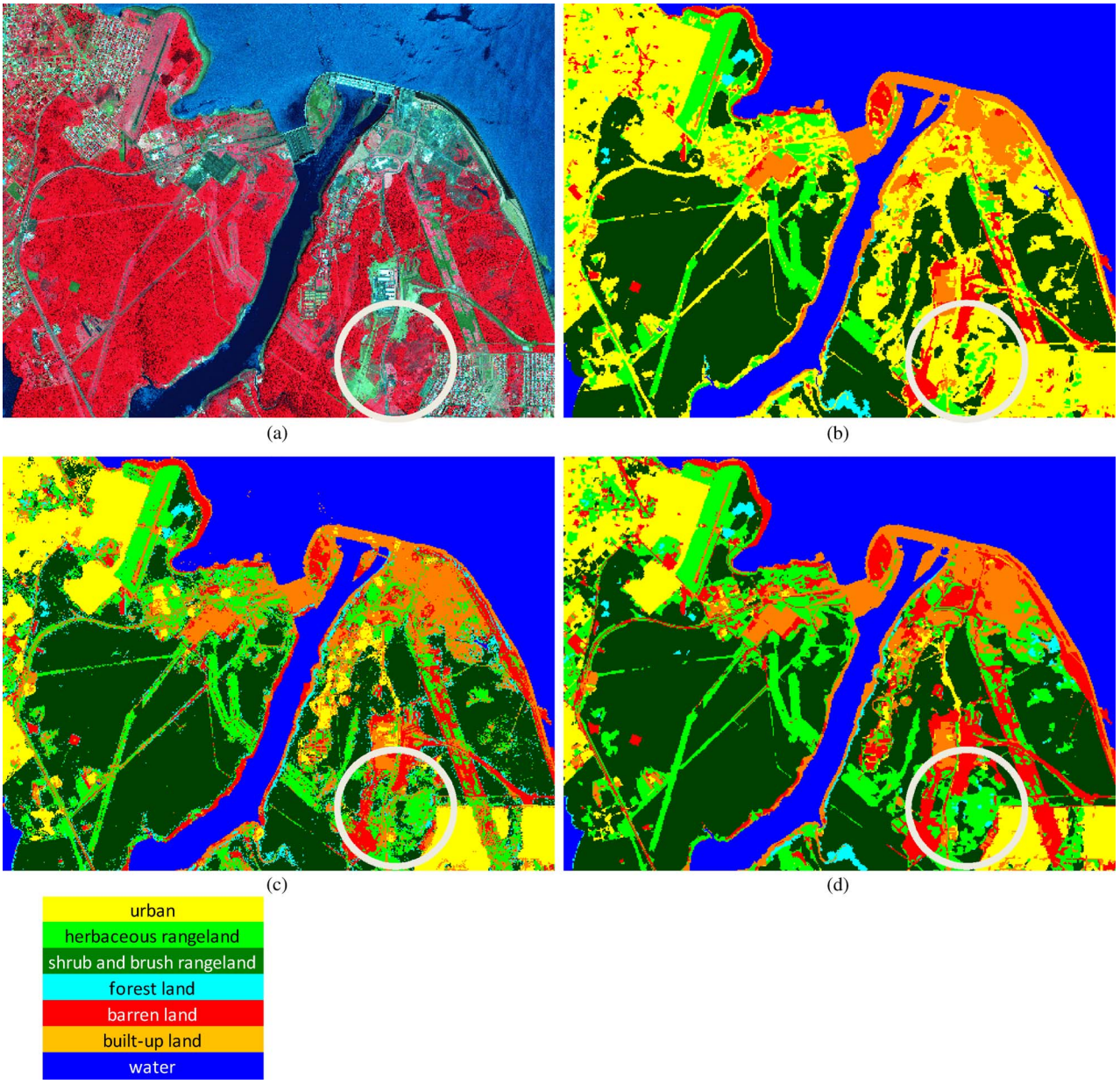

Fig. 5. *"Itaipu" whole image: (a) RGB false-color composition and classification maps obtained (b) by the multiscale Markovian region-based classifier in (5), (c) by a noncontextual classification with both spectral and texture features, and (d) by the extension of the multiscale Markovian region-based classifier with adaptive texture extraction. The white circles highlight an area that is mostly erroneously classified as "urban land" in (b) whereas it is correctly labeled as vegetated in (d).*

semivariogram and SVM in the present experiments can be found in [61]. When applying SVM to both spectral and semivariogram features, a visually good discrimination of textured classes, including the aforementioned vegetated land covers, was obtained but an irregular behavior was also remarked near the edges between different classes, due to the moving-window procedure involved in the computation of the semivariogram [see Fig. 5(c)]. From this perspective, the results in Fig. 5(b) and (c) look complementary to each other.

The application to the whole "Itaipu" image of the iterative algorithm in [61], which combines the multiscale region-based Markovian classifier with textures and adaptively guides the texture extraction according to the class edges, allowed the map in Fig. 5(d) to be obtained. This generalized method intrinsically incorporates neighborhood, segment, and texture information in a unique multiscale algorithm. The resulting classification map correctly discriminated all considered, textured and nontextured, classes and, thanks to adaptive texture extraction, exhibited

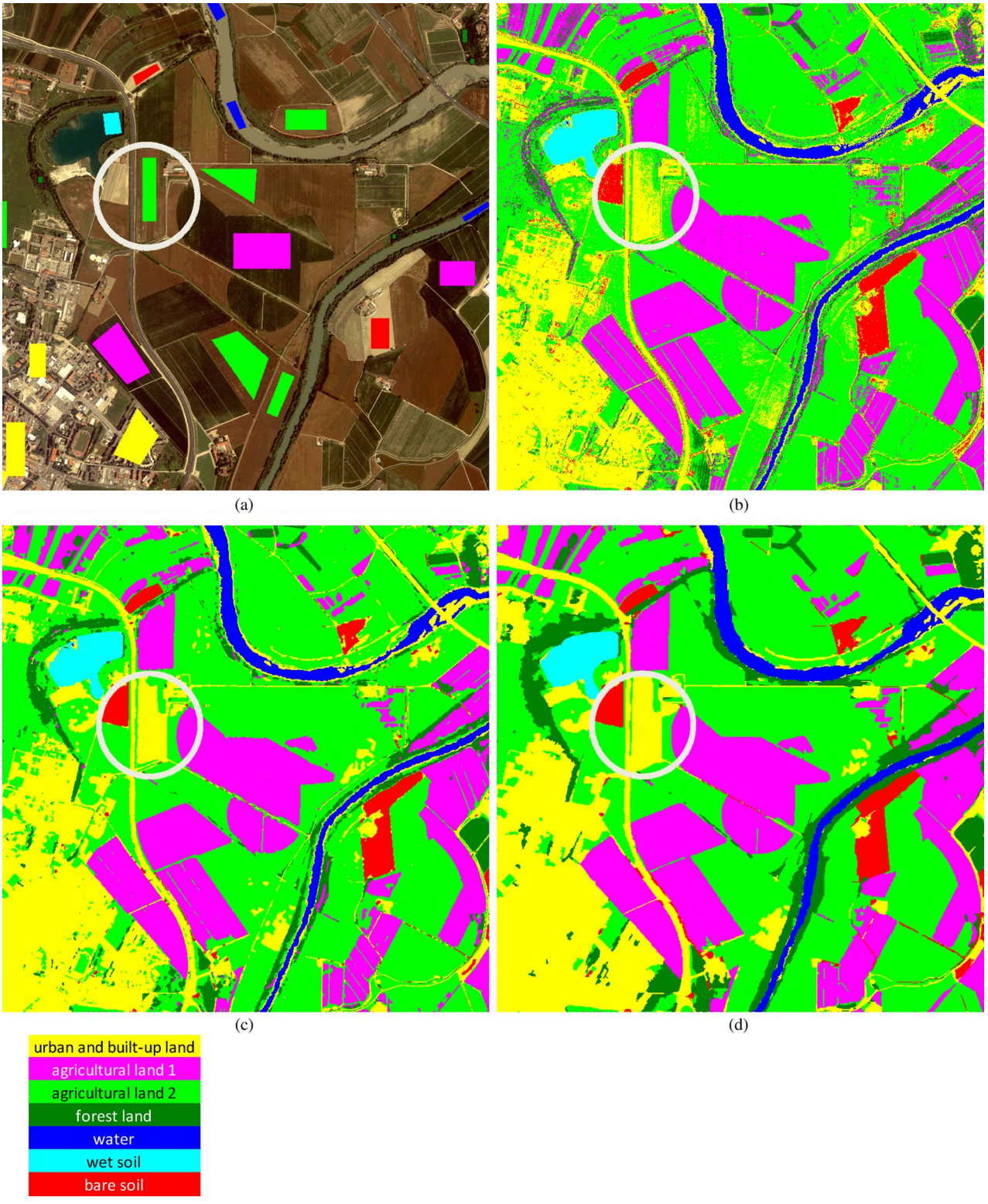

Fig. 6. ***"Alessandria" case study: (a) RGB true-color composition and classification maps obtained (b) by a noncontextual Gaussian Bayesian classifier applied to the spectral channels and (c) by Markovian classifiers based on the Potts model, and (d) on the multiscale region-based model in (5). The white circles highlight an area that is mostly erroneously labeled as "urban and built-up land" in (b)–(d). Test pixels are highlighted in (a).***

no relevant edge artifacts [see Fig. 5(d)]. This confirms the remarkable capability of Markovian techniques of fusing multiple types of contextual information. This capability allows diverse land-cover classes, characterized by textured behaviors as well as by strong spatial–geometrical structures, to be accurately discriminated, and proves that MRFs represent powerful tools in VHR image classification.

As in the case of the image subset, the accuracy of the results in Fig. 5 was also confirmed by a quantitative analysis involving test pixels. Here, we do not detail this analysis, because very accurate classification results (overall accuracies above 99%) were obtained on the test set by all three considered techniques. However, due to the localization of test pixels inside homogeneous areas, relevant differences between the three results were not pointed out by a comparison of the numerical accuracies but, as discussed above, were apparent from a visual analysis of the maps in Fig. 5.

C. Alessandria Case Study

In order to exemplify the results provided by the discussed Markovian approaches, the MRF-based classifiers that use the Potts model, the region-based multiscale approach in (5), and its extension with adaptive texture extraction were also applied to the "Alessandria" data set. Because of the more accurate results obtained with the region-based model in (5) than with the edge-preserving model in (4) (as in the case of "Itaipu"), the results of the latter will not be shown in this second case study. For the sake of comparison, noncontextual methods based on the applications of the Gaussian Bayesian classifier to the spectral channels and of an SVM-based classifier to both spectral and textural features were also used. The classification accuracies obtained on the test pixels, which were collected again by photointerpretation [see Fig. 6(a)] and were disjoint from the training pixels, are reported in Table 2. The experimental setup and the choices in terms of segmentation, energy minimization, MRF parameter optimization, and texture extraction were the same as for "Itaipu."

Quite an accurate classification result was obtained by the noncontextual Gaussian Bayesian classifier (see Table 2) with a nearly 90% overall accuracy. However, a visual inspection of the corresponding map [see Fig. 6(b)] points out, as expected, a noisy spatial behavior, especially in the urban area included in the scene. Furthermore, quite low classification accuracy (below 80%) was obtained for one of the two agricultural land covers, whose pixels were in part erroneously classified as "urban and built-up land" [see, for instance, the circled area in Fig. 6(b)]. The confusion between these two classes is explained by rather similar values of the satellite spectral channels in certain areas of the related land covers and by the resulting overlapping between their probability distributions in the feature space.

Remarkably, the same classification errors can be noted in the results generated by Markovian classifiers with the Potts model and with the region-based multiscale model in (5) without texture features. Such methods yielded, as expected, accuracy improvements as compared to the noncontextual result in Fig. 6(b), increasing the overall and average accuracy of 1%–2% and 6%–8%, respectively. The noisy spatial behavior observed in the result of the noncontextual Gaussian Bayesian classifier was significantly reduced in the result of the Potts-based classifier [see Fig. 6(c)] and removed in the map of the region-based Markovian classifier [see Fig. 6(d)]. However, misclassified agricultural areas can still be remarked in these contextual classification maps, since none of the two approaches can accurately capture the textured spatial behaviors of land covers, unless specific texture features are given in input to them.

A complementary result was obtained by a noncontextual classification with both spectral and textural features. In this case, high classification accuracies were achieved for both agricultural classes (see Table 2) and the resulting overall accuracy was nearly 97%. This is reflected in the corresponding map [see Fig. 7(b)], in which the agricultural areas are visually well discriminated. Nevertheless, artifacts near the class borders and sparse erroneously

Table 2 "Alessandria" Case Study: Classification Accuracies (on the Test Set) of a Noncontextual Gaussian Bayesian Classifier Applied to the Spectral Channels, of Markovian Classifiers Based on the Potts Model, on the Multiscale Region-Based Model in (5), and of Its Variant With Adaptive Texture Extraction, and of a Noncontextual Classifier Applied to Spectral and Textural Features

Land cover class	Non-contextual Gaussian Bayesian classifier	MRF-based classifier with Potts model	MRF- and region-based multiscale classifier	MRF- and region-based multiscale classifier with adaptive texture extraction	Non-contextual classifier with textures
urban and built-up	92.1%	95.0%	98.8%	100%	99.6%
agricultural 1	96.6%	98.8%	99.9%	100%	97.2%
agricultural 2	79.7%	79.2%	77.5%	100%	93.7%
forest	54.5%	94.8%	100%	100%	99.3%
water	99.4%	99.6%	100%	99.9%	99.7%
wet soil	100%	100%	100%	100%	100%
bare soil	99.5%	100%	100%	100%	100%
overall accuracy	89.6%	91.1%	91.6%	100%	96.7%
average accuracy	88.8%	95.3%	96.6%	100%	98.5%

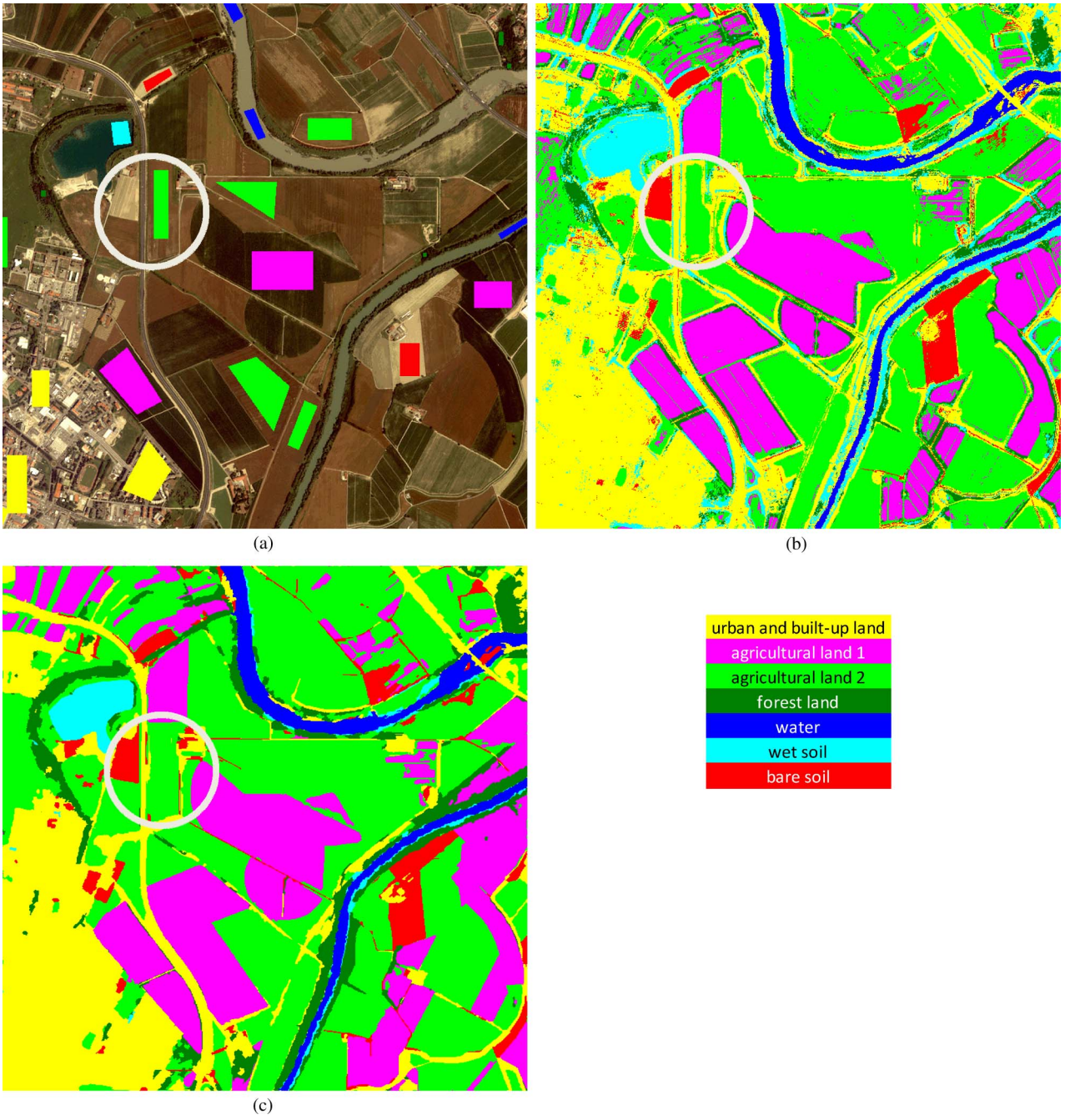

Fig. 7. ***"Alessandria" case study: (a) RGB true-color composition and classification maps obtained (b) by the SVM noncontextual classifier with both satellite observations and texture features and (c) by the Markovian classifier based on the multiscale region-based model in (5) with adaptive texture extraction. The white circles highlight an area, which is classified erroneously when only the spectral channels are used and correctly when texture features are also exploited. Test pixels are highlighted in (a).***

classified pixels can also be noted in this map, an undesired but expected behavior due to the use of a noncontextual classifier and of moving-window procedures in texture extraction. From this perspective, the iterative algorithm in [61], which integrates the region-based MRF model in (5) with adaptive texture extraction, allows the advantages of both approaches to be combined. In the resulting land-cover map [see Fig. 7(c)], all considered land covers were correctly discriminated, including those with well-defined geometrical shapes and those characterized by internal textures. Compared to the result in Fig. 6(d), the use of textures makes it possible to correctly classify all agricultural covers, while keeping the spatial regularity of region-based classification results. Conversely, compared to

noncontextual classification with texture features, the combination with a region-based MRF and the consequent adaptivity in texture extraction, sharply reduce border artifacts. This is reflected in the corresponding almost 100% accuracies of this algorithm on test pixels (see Table 2; we stress again that these are optimistic estimates of the classification performances over the whole image).

V. CONCLUSION

The main issues related to the use of Markov random field models in land-cover mapping from remote sensing images were discussed in this paper, with a special focus on the challenging and topical case of input VHR imagery. In particular, the role of spatial–contextual information in the discrimination of land-cover classes has been discussed by considering the Markovian, region-based, and texture-based approaches to the modeling of this information in land-cover classification techniques. Examples of processing results obtained by classical and advanced Markovian classifiers in the application to two case studies, presenting diverse types of land covers and of spatial image behaviors, have been presented and discussed.

These results have confirmed the remarkable capability of Markov models to integrate together the three aforementioned approaches in a classification task. Region-based and texture-based techniques convey important information to the discrimination of land-cover classes that exhibit rather well-defined geometrical structures and spatially textured behaviors, respectively. Examples of MRF models have been shown in which such approaches are jointly combined in a Markovian framework to support a correct discrimination of arbitrary land-cover classes.

Born as rigorous stochastic models for the contextual information associated with image data, Markov random fields currently play a primary role also as data-fusion tools, able to incorporate multiple information sources (e.g., deriving from multisensor, multiscale, multichannel, or multitemporal input data) for the classification purpose. This flexibility is mostly obtained through the formalization of Markov models in terms of energy functions (an opportunity ensured by the analytical theory of MRFs over pixel lattices) and through the proper design of the energy that best fits the characteristics of each classification problem in terms of resolution, input data distribution, and spatial statistics. A typical strategy to define this energy for a given VHR image-classification problem is first to formalize each input information source (e.g., each sensor or spatial scale) by computing an energy contribution according to the spatial behaviors of the classes (e.g., presence of geometrical structures or of textures) and to corresponding spatial descriptors (e.g., edges, segments, or texture features). Then, these separate energy contributions can be linearly combined in a comprehensive energy function to be minimized in order to generate the output classification map.

As suggested also by the presented experimental results, advanced Markovian models currently allow high classification accuracies to be obtained in land-cover mapping also from challenging remote sensing data sets. The collection of the considered MRF-based classifiers ranged from the use of the classical Potts MRF model to recent techniques involving edge modeling through line processes, multiscale segment information, and adaptive texture extraction. The subtasks of edge detection, segmentation, and texture analysis have been addressed by applying or adapting the Canny edge detector, the graph-based segmentation method in [103], and the semivariogram texture extractor, respectively [59]–[61]. However, essentially arbitrary edge detection, multiscale segmentation, and texture analysis methods could be plugged in the considered Markovian classifiers. Additional experiments (not discussed for brevity) also suggested: 1) a limited sensitivity of the method in [60] to the input edge map, provided this map detected (even though with low accuracy) the main borders among the land-cover classes and did not include too many edges inside each class; 2) a remarkable robustness of the method in [59] to a reduction in the number of scales, provided that, at least, the coarsest and finest scale segmentations are used; and 3) a rather limited sensitivity of the method in [61] to the values of the number of scales and to the size of the moving window used for texture analysis (more details can be found in [59]–[61]).

Despite the intrinsic conceptual complexity of these recent MRF models, their use can require little, if any, effort to the user, thanks to the current availability of efficient techniques for automatic parameter optimization. These favorable features are also supported both by the current advances in hardware and computing resources and by the availability of recent computationally efficient techniques, such as graph cuts, to address the intensive optimization problems involved in MRF-based processing. Thanks to these methodological and computational properties, Markov random fields currently represent a scientifically mature approach in the framework of remote sensing image analysis. This explains the increasing popularity of these models in diverse applications, including denoising, multitemporal image analysis, and change detection. More generally, this current role of Markov models is consistent with the scientific maturity of the field of remote sensing image analysis, rooted in the disciplines of pattern recognition and image processing, that presently allows the potential for classification, segmentation, and feature-extraction techniques to be exploited not only for laboratory experiments but also for practical and operational applications.

A currently important technical and scientific challenge is to drive further the development of the scientific field of Markov models for remote sensing image classification, by proposing novel accurate and reliable models and methods, for instance, by combining MRFs with currently interesting approaches such as SVMs [24], [104] and

mathematical morphology [71]. Keeping this scientific field continuously updated is a pivotal effort, while new sensors and satellite missions, new types of remote sensing data (e.g., with further improved spatial resolutions), new input information sources (e.g., wireless sensor networks), and new computing capabilities (e.g., graphical processing units or cloud computing) become available. An important issue is also to encourage the diffusion of MRF-based processing tools in applicative contexts, in which simpler but often suboptimal approaches tend to consolidate in the usual practice, to take advantage of the flexibility and accuracy that these powerful tools offer in the extraction of information from remote sensing imagery. ■

Acknowledgment

The authors would like to thank Dr. M. De Martino for her help in the experiments and Dr. F. Causa, M. Pirozzi, L. Peruzzo, and M. Tognoni for their contributions to implementation.

REFERENCES

[1] J. Richards and X. Jia, *Remote Sensing Digital Image Analysis*. New York: Springer-Verlag, 2005.

[2] R. O. Duda, P. E. Hart, and D. G. Stork, *Pattern Classification*, 2nd ed. New York: Wiley, 2001.

[3] V. Madhok and D. A. Landgrebe, "A process model for remote sensing data analysis," *IEEE Trans. Geosci. Remote Sens.*, vol. 40, no. 3, pp. 680–686, Mar. 2002.

[4] C. M. Bishop, *Neural Networks for Pattern Recognition*. Oxford, U.K.: Oxford Univ. Press, 1995.

[5] J. C. Bezdek, *Pattern Recognition With Fuzzy Objective Function Algorithms*. Norwell, MA: Kluwer, 1981.

[6] V. N. Vapnik, *The Nature of Statistical Learning Theory*. New York: Springer-Verlag, 1995.

[7] L. I. Kuncheva, *Combining Pattern Classifiers: Methods and Algorithms*. New York: Wiley, 2004.

[8] W. K. Pratt, *Digital Image Processing*. New York: Wiley, 1991.

[9] F. Causa, G. Moser, and S. B. Serpico, "A novel MRF model for the detection of urban areas in optical high spatial resolution images," *Rivista Italiana di Telerilevamento*, vol. 38, pp. 59–72, 2007.

[10] S. Z. Li, *Markov Random Field Modeling in Image Analysis*. New York: Springer-Verlag, 2010.

[11] H. Derin and P. A. Kelly, "Discrete-index Markov-type random processes," *Proc. IEEE*, vol. 77, no. 10, pp. 1485–1510, Oct. 1989.

[12] L. Schrage, "Queueing systems, Vol. I: Theory," *Proc. IEEE*, vol. 65, no. 6, pp. 990–991, Jun. 1977.

[13] D. I. Shuman, A. Nayyar, A. Mahajan, Y. Goykhman, K. Li, M. Liu, D. Teneketzis, M. Moghaddam, and D. Entekhabi, "Measurement scheduling for soil moisture sensing: From physical models to optimal control," *Proc. IEEE*, vol. 98, no. 11, pp. 1918–1933, Nov. 2010.

[14] E. Costamagna, L. Favalli, and P. Gamba, "Multipath channel modeling with chaotic attractors," *Proc. IEEE*, vol. 90, no. 5, pp. 842–859, May 2002.

[15] L. R. Rabiner, "A tutorial on hidden Markov models and selected applications in speech recognition," *Proc. IEEE*, vol. 77, no. 2, pp. 257–286, Feb. 1989.

[16] S. J. Godsill, J. Vermaak, W. Ng, and J. F. Li, "Models and algorithms for tracking of maneuvering objects using variable rate particle filters," *Proc. IEEE*, vol. 95, no. 5, pp. 925–952, May 2007.

[17] Y. Lecun, L. Bottou, Y. Bengio, and P. Haffner, "Gradient-based learning applied to document recognition," *Proc. IEEE*, vol. 86, no. 11, pp. 2278–2324, Nov. 1998.

[18] M. Kunt, "A statistical model for correlation functions of two-level digital facsimiles," *Proc. IEEE*, vol. 63, no. 2, pp. 327–329, Feb. 1975.

[19] T. Ozcelik, J. C. Brailean, and A. K. Katsaggelos, "Image and video compression algorithms based on recovery techniques using mean field annealing," *Proc. IEEE*, vol. 83, no. 2, pp. 304–316, Feb. 1995.

[20] S. Geman and D. Geman, "Stochastic relaxation, Gibbs distributions, and the Bayesian restoration of images," *IEEE Trans. Pattern Anal. Mach. Intell.*, vol. PAMI-6, no. 6, pp. 721–741, Jun. 1984.

[21] R. C. Dubes and A. K. Jain, "Random field models in image analysis," *J. Appl. Stat.*, vol. 16, no. 2, pp. 131–164, 1989.

[22] A. H. S. Solberg, T. Taxt, and A. K. Jain, "A Markov random field model for classification of multisource satellite imagery," *IEEE Trans. Geosci. Remote Sens.*, vol. 34, no. 1, pp. 100–113, Jan. 1996.

[23] S. B. Serpico and G. Moser, "Weight parameter optimization by the Ho-Kashyap algorithm in MRF models for supervised image classification," *IEEE Trans. Geosci. Remote Sens.*, vol. 44, no. 12, pp. 3695–3705, Dec. 2006.

[24] Y. Tarabalka, M. Fauvel, J. Chanussot, and J. A. Benediktsson, "SVM- and MRF-based method for accurate classification of hyperspectral images," *IEEE Geosci. Remote Sens. Lett.*, vol. 7, no. 4, pp. 736–740, Oct. 2010.

[25] Q. Jackson and D. Landgrebe, "Adaptive Bayesian contextual classification based on Markov random fields," *IEEE Trans. Geosci. Remote Sens.*, vol. 40, no. 11, pp. 2454–2463, Nov. 2002.

[26] V. Krylov, G. Moser, S. B. Serpico, and J. Zerubia, "Supervised high resolution dual polarization SAR image classification by finite mixtures and copulas," *IEEE J. Sel. Topics Signal Process.*, vol. 5, no. 3, pp. 554–566, Jun. 2011.

[27] G. Poggi, G. Scarpa, and J. Zerubia, "Supervised segmentation of remote sensing images based on a tree-structured MRF model," *IEEE Trans. Geosci. Remote Sens.*, vol. 43, no. 8, pp. 1901–1911, Aug. 2005.

[28] H. Deng and D. A. Clausi, "Unsupervised segmentation of synthetic aperture radar sea ice imagery using a novel Markov random field model," *IEEE Trans. Geosci. Remote Sens.*, vol. 43, no. 3, pp. 528–538, Mar. 2005.

[29] P. C. Smits and S. G. Dellepiane, "Synthetic aperture radar image segmentation by a detail preserving Markov random field approach," *IEEE Trans. Geosci. Remote Sens.*, vol. 35, no. 4, pp. 844–857, Jul. 1997.

[30] M. Soccorsi, D. Gleich, and M. Datcu, "Huber-Markov model for complex SAR image restoration," *IEEE Geosci. Remote Sens. Lett.*, vol. 7, no. 1, pp. 63–67, Jan. 2010.

[31] M. Walessa and M. Datcu, "Model-based despeckling and information extraction from SAR images," *IEEE Trans. Geosci. Remote Sens.*, vol. 38, no. 5, pp. 2258–2269, May 2000.

[32] M. Mignotte, "A multiresolution Markovian fusion model for the color visualization of hyperspectral images," *IEEE Trans. Geosci. Remote Sens.*, vol. 48, no. 12, pp. 4236–4247, Dec. 2010.

[33] G. Rellier, X. Descombes, F. Falzon, and J. Zerubia, "Texture feature analysis using a Gauss-Markov model in hyperspectral image classification," *IEEE Trans. Geosci. Remote Sens.*, vol. 42, no. 7, pp. 1543–1551, Jul. 2004.

[34] S. Urago, J. Zerubia, and M. Berthod, "Markovian model for contour grouping," *Pattern Recognit.*, vol. 28, no. 5, pp. 683–693, 1995.

[35] M. Negri, P. Gamba, G. Lisini, and F. Tupin, "Junction-aware extraction and regularization of urban road networks in high-resolution SAR images," *IEEE Trans. Geosci. Remote Sens.*, vol. 44, no. 10, pp. 2962–2971, Oct. 2006.

[36] H. Shekarforoush, M. Berthod, J. Zerubia, and M. Werman, "Sub-pixel Bayesian estimation of albedo and height," *Int. J. Comput. Vis.*, vol. 19, no. 3, pp. 289–300, 1996.

[37] G. Moser and S. B. Serpico, "Unsupervised change detection from multichannel SAR data by Markovian data fusion," *IEEE Trans. Geosci. Remote Sens.*, vol. 47, no. 7, pp. 2114–2128, Jul. 2009.

[38] G. Moser, S. B. Serpico, and G. Vernazza, "Unsupervised change detection from multichannel SAR images," *IEEE Geosci. Remote Sens. Lett.*, vol. 4, no. 2, pp. 278–282, Apr. 2007.

[39] G. Moser, E. Angiati, and S. B. Serpico, "Multiscale unsupervised change detection on optical images by Markov random fields and wavelets," *IEEE Geosci. Remote Sens. Lett.*, vol. 8, no. 4, pp. 725–729, Jul. 2011.

[40] L. Bruzzone and D. Fernandez Prieto, "Automatic analysis of the difference image for unsupervised change detection," *IEEE Trans. Geosci. Remote Sens.*, vol. 38, no. 3, pp. 1171–1182, Mar. 2000.

[41] F. Melgani and S. B. Serpico, "A Markov random field approach to spatio-temporal contextual image classification," *IEEE Trans. Geosci. Remote Sens.*, vol. 41, no. 11, pp. 2478–2487, Nov. 2003.

[42] L. Gueguen and M. Datcu, "Image time-series data mining based on the information-bottleneck principle," *IEEE*

Trans. Geosci. Remote Sens., vol. 45, no. 4, pp. 827–838, Apr. 2007.

[43] G. Ferraiuolo and V. Pascazio, "The effect of modified Markov random fields on the local minima occurrence in microwave imaging," *IEEE Trans. Geosci. Remote Sens.*, vol. 41, no. 5, pp. 1043–1055, May 2003.

[44] G. Ferraiuolo, V. Pascazio, and G. Schirinzi, "Maximum a posteriori estimation of height profiles in InSAR imaging," *IEEE Geosci. Remote Sens. Lett.*, vol. 1, no. 2, pp. 66–70, Apr. 2004.

[45] F. Tupin and M. Roux, "Markov random field on region adjacency graph for the fusion of SAR and optical data in radargrammetric applications," *IEEE Trans. Geosci. Remote Sens.*, vol. 43, no. 8, pp. 1920–1928, Aug. 2005.

[46] X. Min, H. Chen, and P. K. Varshney, "An image fusion approach based on Markov random fields," *IEEE Trans. Geosci. Remote Sens.*, vol. 49, no. 12, pp. 5116–5127, Dec. 2011.

[47] R. Nishii, "A Markov random field-based approach to decision-level fusion for remote sensing image classification," *IEEE Trans. Geosci. Remote Sens.*, vol. 41, no. 10, pp. 2316–2319, Oct. 2003.

[48] A. Katartzis and H. Sahli, "A stochastic framework for the identification of building rooftops using a single remote sensing image," *IEEE Trans. Geosci. Remote Sens.*, vol. 46, no. 1, pp. 259–271, Jan. 2008.

[49] M. M. Daniel and A. S. Willsky, "A multiresolution methodology for signal-level fusion and data assimilation with applications to remote sensing," *Proc. IEEE*, vol. 85, no. 1, pp. 164–180, Jan. 1997.

[50] T. Kasetkasem, M. K. Arora, and P. K. Varshney, "Super-resolution land cover mapping using a Markov random field based approach," *Remote Sens. Environ.*, vol. 96, no. 3–4, pp. 302–314, 2005.

[51] F. Li, X. Jia, D. Fraser, and A. Lambert, "Super resolution for remote sensing images based on a universal hidden Markov tree model," *IEEE Trans. Geosci. Remote Sens.*, vol. 48, no. 3, pp. 1270–1278, Mar. 2010.

[52] D. M. Greig, B. T. Porteous, and A. H. Seheult, "Exact maximum a posteriori estimation for binary images," *J. Roy. Stat. Soc. B*, vol. 51, pp. 271–279, 1989.

[53] V. Kolmogorov and R. Zabih, "What energy functions can be minimized via graph cuts?" *IEEE Trans. Pattern Anal. Mach. Intell.*, vol. 26, no. 2, pp. 147–159, Feb. 2004.

[54] Z. Kato, M. Berthod, and J. Zerubia, "Hierarchical Markov random field model and multitemperature annealing for parallel image classification," *Graph. Models Image Process.*, vol. 58, no. 1, pp. 18–37, 1996.

[55] G. O. Storvik, R. Fjørtoft, and A. H. S. Solberg, "A Bayesian approach to classification of multi-scale remote sensing data," *IEEE Trans. Geosci. Remote Sens.*, vol. 43, no. 3, pp. 539–547, Mar. 2005.

[56] A. S. Willsky, "Multiresolution Markov models for signal and image processing," *Proc. IEEE*, vol. 90, no. 8, pp. 1396–1458, Aug. 2002.

[57] J.-M. Laferté, P. Pérez, and F. Heitz, "Discrete Markov image modeling and inference on the quadtree," *IEEE Trans. Image Process.*, vol. 9, no. 3, pp. 390–404, Mar. 2000.

[58] C. A. Bouman and M. Shapiro, "A multiscale random field model for Bayesian image segmentation," *IEEE Trans. Image Process.*, vol. 3, no. 2, pp. 162–177, Mar. 1994.

[59] G. Moser and S. B. Serpico, "Classification of high-resolution images based on MRF fusion and multiscale segmentation," in *Proc. IEEE Geosci. Remote Sens. Symp.*, Boston, MA, 2008, vol. II, pp. 277–280.

[60] G. Moser and S. B. Serpico, "Edge-preserving classification of high-resolution remote-sensing images by Markovian data fusion," in *Proc. IEEE Geosci. Remote Sens. Symp.*, Capetown, South Africa, 2009, vol. IV, pp. 765–768.

[61] G. Moser and S. B. Serpico, "Contextual high-resolution image classification by Markovian data fusion, adaptive texture extraction, and multiscale segmentation," in *Proc. IEEE Geosci. Remote Sens. Symp.*, Vancouver, BC, Canada, 2011, pp. 1155–1158.

[62] M. Schroder, H. Rehrauer, K. Seidel, and M. Datcu, "Spatial information retrieval from remote-sensing images. II. Gibbs-Markov random fields," *IEEE Trans. Geosci. Remote Sens.*, vol. 36, no. 5, pp. 1446–1455, May 1998.

[63] C.-H. Chen and P.-G. P. Ho, "Statistical pattern recognition in remote sensing," *Pattern Recognit.*, vol. 41, no. 9, pp. 2731–2741, 2008.

[64] H. Fizazi Izabatene and R. Rabahi, "Classification of remote sensing data with Markov random field," *J. Appl. Sci.*, vol. 10, no. 8, pp. 636–643, 2010.

[65] S. B. Serpico and G. Moser, "MRF-based remote-sensing image classification with automatic model-parameter estimation," in *Signal and Image Processing for Remote Sensing*, C. H. Chen, Ed. London, U.K.: Taylor & Francis/CRC Press, 2006, pp. 305–326.

[66] R. Haralick, K. Shanmugam, and I. Dinstein, "Textural features for image classification," *IEEE Trans. Syst. Man Cybern.*, vol. SMC-3, no. 6, pp. 610–621, Nov. 1973.

[67] G. Forzieri, G. Moser, E. R. Vivoni, F. Castelli, and F. Canovaro, "Riparian vegetation mapping for hydraulic roughness estimation using very high resolution remote sensing data fusion," *J. Hydraul. Eng.*, vol. 136, pp. 855–867, 2010.

[68] Q. Chen and P. Gong, "Automatic variogram parameter extraction for textural classification of the panchromatic IKONOS imagery," *IEEE Trans. Geosci. Remote Sens.*, vol. 42, no. 5, pp. 1106–1115, May 2004.

[69] J. A. Benediktsson, M. Pesaresi, and K. Amason, "Classification and feature extraction for remote sensing images from urban areas based on morphological transformations," *IEEE Trans. Geosci. Remote Sens.*, vol. 41, no. 9, pt. 1, pp. 1940–1949, Sep. 2003.

[70] J. Chanussot, J. A. Benediktsson, and M. Fauvel, "Classification of remote sensing images from urban areas using a fuzzy possibilistic model," *IEEE Trans. Geosci. Remote Sens.*, vol. 3, no. 1, pp. 40–44, Jan. 2006.

[71] M. Fauvel, J. A. Benediktsson, J. Chanussot, and J. R. Sveinsson, "Spectral and spatial classification of hyperspectral data using SVMs and morphological profiles," *IEEE Trans. Geosci. Remote Sens.*, vol. 46, no. 11, pt. 2, pp. 3804–3814, Nov. 2008.

[72] M. Pesaresi and J. A. Benediktsson, "A new approach for the morphological segmentation of high-resolution satellite imagery," *IEEE Trans. Geosci. Remote Sens.*, vol. 39, no. 2, pp. 309–320, Feb. 2001.

[73] M. Dalla Mura, J. A. Benediktsson, B. Waske, and L. Bruzzone, "Morphological attribute profiles for the analysis of very high resolution images," *IEEE Trans. Geosci. Remote Sens.*, vol. 48, no. 10, pp. 3747–3762, Oct. 2010.

[74] S. Mallat, "Wavelets for a vision," *Proc. IEEE*, vol. 84, no. 4, pp. 604–614, Apr. 1996.

[75] X. Zhang, N. H. Younan, and C. G. O'Hara, "Wavelet domain statistical hyperspectral soil texture classification," *IEEE Trans. Geosci. Remote Sens.*, vol. 43, no. 3, pp. 615–618, Mar. 2005.

[76] M. Shi and G. Healey, "Hyperspectral texture recognition using a multiscale opponent representation," *IEEE Trans. Geosci. Remote Sens.*, vol. 41, no. 5 pp. 1090–1095, May 2003.

[77] T. Blaschke, S. Lang, and G. Hay, Eds., *Object-Based Image Analysis*. New York: Springer-Verlag, 2008.

[78] J. K. Udupa and P. K. Saha, "Fuzzy connectedness and image segmentation," *Proc. IEEE*, vol. 91, no. 10, pp. 1649–1669, Oct. 2003.

[79] S. G. Dellepiane, F. Fontana, and G. L. Vernazza, "Nonlinear image labeling for multivalued segmentation," *IEEE Trans. Image Process.*, vol. 5, no. 3, pp. 429–446, Mar. 1996.

[80] L. Shafarenko, M. Petrou, and J. Kittler, "Automatic watershed segmentation of randomly textured color images," *IEEE Trans. Image Process.*, vol. 6, no. 11, pp. 1530–1544, Nov. 1997.

[81] G. Troglio, J. Le Moigne, J. A. Benediktsson, G. Moser, and S. B. Serpico, "Automatic extraction of ellipsoidal features for planetary image registration," *IEEE Geosci. Remote Sens. Lett.*, vol. 9, no. 1, pp. 95–99, Jan. 2012.

[82] C. D'Elia, G. Scarpa, and G. Poggi, "A tree-structured Markov random field model for Bayesian image segmentation," *IEEE Trans. Image Process.*, vol. 12, no. 10, pp. 1259–1273, Oct. 2003.

[83] J. C. Tilton, "Analysis of hierarchically related image segmentations," in *Proc. IEEE Workshop Adv. Tech. Anal. Remotely Sensed Data*, Greenbelt, MD, Oct. 27–28, 2003, pp. 60–69.

[84] Y. Tarabalka, J. Chanussot, and J. A. Benediktsson, "Segmentation and classification of hyperspectral images using minimum spanning forest grown from automatically selected markers," *IEEE Trans. Syst. Man Cybern. B, Cybern.*, vol. 40, no. 5, pp. 1267–1279, Oct. 2010.

[85] R. Kindermann and J. L. Snell, *Markov Random Fields and Their Applications*. Providence, RI: AMS, 1980.

[86] J. Benediktsson and I. Kanellopoulos, "Classification of multisource and hyperspectral data based on decision fusion," *IEEE Trans. Geosci. Remote Sens.*, vol. 37, no. 3, pp. 1367–1377, Mar. 1999.

[87] A. Bendjebbour, Y. Delignon, L. Fouque, V. Samson, and W. Pieczynski, "Multisensor image segmentation using Dempster-Shafer fusion in Markov fields context," *IEEE Trans. Geosci. Remote Sens.*, vol. 39, no. 8, pp. 1789–1798, Aug. 2001.

[88] H. H. Szu and R. L. Hartley, "Nonconvex optimization by fast simulated annealing," *Proc. IEEE*, vol. 75, no. 11, pp. 1538–1540, Nov. 1987.

[89] J. Besag, "On the statistical analysis of dirty pictures," *J. Roy. Stat. Soc.*, vol. 68, pp. 259–302, 1986.

[90] S. Le Hegarat-Mascle, A. Kallel, and X. Descombes, "Ant colony optimization

for image regularization based on a nonstationary Markov modeling," *IEEE Trans. Image Process.*, vol. 16, no. 3, pp. 865–878, Mar. 2007.

[91] B. Zhang, S. Li, X. Jia, L. Gao, and M. Peng, "Adaptive Markov random field approach for classification of hyperspectral imagery," *IEEE Geosci. Remote Sens. Lett.*, vol. 8, no. 5, pp. 973–977, Sep. 2011.

[92] X. Jia and J. A. Richards, "Cluster-space representation for hyperspectral data classification," *IEEE Trans. Geosci. Remote Sens.*, vol. 40, no. 3, pp. 593–598, Mar. 2002.

[93] M. V. Ibanez and A. Simò, "Parameter estimation in Markov random field image modeling with imperfect observations. A comparative study," *Pattern Recognit. Lett.*, vol. 24, no. 14, pp. 2377–2389, 2003.

[94] X. Descombes, M. Sigelle, and F. Preteux, "Estimating Gaussian Markov random field parameters in a nonstationary framework: Application to remote sensing imaging," *IEEE Trans. Image Process.*, vol. 8, no. 4, pp. 490–503, Apr. 1999.

[95] S. S. Saquib, C. A. Bouman, and K. Sauer, "ML parameter estimation for Markov random fields with applications to Bayesian tomography," *IEEE Trans. Image Process.*, vol. 7, no. 7, pp. 1029–1044, Jul. 1998.

[96] X. Descombes, R. D. Morris, J. Zerubia, and M. Berthod, "Estimation of Markov random field prior parameters using Markov chain Monte Carlo maximum likelihood," *IEEE Trans. Image Process.*, vol. 8, no. 7, pp. 954–963, Jul. 1999.

[97] G. Celeux, F. Forbes, and N. Peyrand, "EM procedures using mean field-like approximations for Markov model-based image segmentation," *Pattern Recognit.*, vol. 36, no. 1, pp. 131–144, 2003.

[98] F. Salzenstein and W. Pieczynski, "Parameter estimation in hidden fuzzy Markov random fields and image segmentation," *Graph. Models Image Process.*, vol. 59, no. 4, pp. 205–220, 1997.

[99] H. Derin and H. Elliott, "Modeling and segmentation of noisy and textured images using Gibbs random fields," *IEEE Trans. Pattern Anal. Mach. Intell.*, vol. PAMI-9, no. 1, pp. 29–55, Jan. 1987.

[100] B. C. K. Tso and P. M. Mather, "Classification of multisource remote sensing imagery using a genetic algorithm and Markov random fields," *IEEE Trans. Geosci. Remote Sens.*, vol. 37, no. 3, pp. 1255–1260, Mar. 1999.

[101] X. Jia and J. A. Richards, "Managing the spectral-spatial mix in context classification using Markov random fields," *IEEE Geosci. Remote Sens. Lett.*, vol. 5, no. 2, pp. 311–314, Apr. 2008.

[102] Y. F. Wong and E. C. Posner, "A new clustering algorithm applicable to multispectral and polarimetric SAR images," *IEEE Trans. Geosci. Remote Sens.*, vol. 31, no. 3, pp. 634–644, Mar. 1993.

[103] P. F. Felzenszwalb and D. Huttenlocherm, "Efficient graph-based image segmentation," *Int. J. Comput. Vis.*, vol. 59, pp. 167–181, 2004.

[104] G. Moser and S. B. Serpico, "Contextual remote-sensing image classification by support vector machines and Markov random fields," in *Proc. IEEE Geosci. Remote Sens. Symp.*, Honolulu, HI, 2010, pp. 3728–3731.

[105] F. Melgani and S. B. Serpico, "A statistical approach to the fusion of the spectral and spatio-temporal contextual information for the classification of remote sensing images," *Pattern Recognit. Lett.*, vol. 23, no. 9, pp. 1053–1061, 2002.

ABOUT THE AUTHORS

Gabriele Moser (Member, IEEE) received the Laurea degree (M.Sc. equivalent; *summa cum laude*) in telecommunications engineering and the Ph.D. degree in space sciences and engineering from the University of Genoa, Genoa, Italy, in 2001 and 2005, respectively.

Since 2010, he has been an Assistant Professor of Telecommunications at the University of Genoa. Since 2001, he has cooperated with the Signal Processing and Telecommunications Research Laboratory of the University of Genoa. From January to March 2004, he was a visiting student at the Institut National de Recherche en Informatique et en Automatique (INRIA), Sophia Antipolis, France. His research activity is focused on the development of image processing and pattern recognition methodologies for remote sensing data interpretation. His current research interests include contextual classification, multitemporal image classification and change detection, SAR data analysis, hyperspectral image classification, and geo/biophysical parameter estimation.

Dr. Moser has been a reviewer for several international journals. He has been an Associate Editor of the IEEE Geoscience and Remote Sensing Letters and *Pattern Recognition Letters* since 2008 and 2011, respectively.

Sebastiano B. Serpico (Fellow, IEEE) received the Laurea degree in electronic engineering and the Ph.D. degree from the University of Genoa, Genoa, Italy, in 1982 and 1989, respectively.

He is a Full Professor of Telecommunications at the Faculty of Engineering, University of Genoa, and the Head of the Signal Processing and Telecommunications Laboratory of the Department of Telecommunications, Electronic, Electrical, and Naval Engineering, University of Genoa. His current research interests include pattern recognition for remote sensing images and for biomedical images. He has been the project manager of numerous research contracts and an evaluator of project proposals for various programs of the European Union. He is author (or coauthor) of more than 200 scientific articles published in journals and conference proceedings.

Prof. Serpico is the Chairman of the Institute of Advanced Studies in Information and Communication Technologies (ISICT). He is an Associate Editor of the IEEE Transactions on Geoscience and Remote Sensing. He was a Guest Editor of two Special Issues of the IEEE Transactions on Geoscience and Remote Sensing on the subject of the "Analysis of Hyperspectral Image Data" (July 2001) and on the subject "Advances in Techniques for the Analysis of Remote Sensing Data" (March 2005). From 1998 to 2002, he was the Chairman of a SPIE/EUROPTO series of conferences on Signal and Image Processing for Remote Sensing.

Jón Atli Benediktsson (Fellow, IEEE) received the Cand.Sci. degree in electrical engineering from the University of Iceland, Reykjavik, Iceland, in 1984 and the M.S.E.E. and Ph.D. degrees from Purdue University, West Lafayette, IN, in 1987 and 1990, respectively.

Currently, he is Pro Rector of Academic Affairs and Professor of Electrical and Computer Engineering at the University of Iceland. His research interests are in remote sensing, image analysis, pattern recognition, biomedical analysis of signals, and signal processing, and he has published extensively in those fields. He is a cofounder of the biomedical startup company Oxymap.

Prof. Benediktsson is the 2011–2012 President of the IEEE Geoscience and Remote Sensing Society (GRSS) and has been on the GRSS Administrative Committee since 2000. He was the Editor of the IEEE Transactions on Geoscience and Remote Sensing (TGRS) from 2003 to 2008 and has served as an Associate Editor of TGRS since 1999 and the IEEE Geoscience and Remote Sensing Letters since 2003. He received the Stevan J. Kristof Award from Purdue University in 1991 as outstanding graduate student in remote sensing. In 1997, he was the recipient of the Icelandic Research Council's Outstanding Young Researcher Award; in 2000, he was granted the IEEE Third Millennium Medal; in 2004, he was a corecipient of the University of Iceland's Technology Innovation Award; in 2006, he received the yearly research award from the Engineering Research Institute of the University of Iceland; and in 2007, he received the Outstanding Service Award from the IEEE Geoscience and Remote Sensing Society. He is corecipient of the 2012 IEEE Transactions on Geoscience and Remote Sensing Best Paper Award. He is a member of Societas Scientiarum Islandica and Tau Beta Pi.